TOPOOPT: Optimizing the Network Topology for Distributed DNN Training

Weiyang Wang[1]   Moein Khazraee[1]   Zhizhen Zhong[1]   Zhijao Jia[2,3]
Dheevatsa Mudigere[3]   Ying Zhang[3]   Anthony Kewitsch[4]   Manya Ghobadi[1]

[1]Massachusetts Institute of Technology   [2]CMU   [3]Facebook   [4]Telescent

Abstract

We explore a novel approach for building DNN training clusters using commodity optical devices. Our proposal, called TOPOOPT, co-optimizes the distributed training process across three dimensions: computation, communication, and network topology. TOPOOPT uses a novel alternating optimization technique and a group theory-inspired algorithm to find the best network topology and routing plan, together with parallelization strategy, for distributed DNN training. To motivate our proposal, we measure the communication patterns of distributed DNN workloads at a large online service provider. Experiments with a 12-node prototype demonstrate the feasibility of TOPOOPT. Simulations on real distributed training models show that, compared to similar-cost Fat-tree interconnects, TOPOOPT reduces DNN training time by up to $3\times$.

1 Introduction

Our society is rapidly becoming reliant on deep neural networks (DNNs). New datasets and models are invented frequently, increasing the memory and computational requirements for training. This explosive growth has created an urgent demand for efficient distributed DNN training systems.

Today's DNN training systems are built on top of traditional datacenter clusters, with electrical packet switches arranged in a multi-tier Fat-tree topology [45]. Fat-tree topologies are traffic oblivious fabrics, allowing uniform bandwidth and latency between server pairs. They are ideal when the workload is unpredictable and consists mostly of short transfers–two inherent properties of legacy datacenter workloads [47, 48, 51, 63, 64]. However, Fat-tree networks are becoming a bottleneck for distributed DNN training workloads [55, 65, 71, 76, 90, 93, 116].

Prior work has focused on addressing this challenge by reducing the size of parameters to transmit through the network [46, 55, 56, 65, 69, 73–75, 82, 93, 105, 119] and developing techniques to discover faster parallelization strategies while considering the available network bandwidth [44, 46, 76, 93, 109]. These proposals co-optimize computation and communication as two important dimensions of distributed DNN training, but they do not consider the *physical layer topology* as an optimization dimension.

Recently, SiP-ML [79] demonstrated the benefits of 8 Tbps silicon photonics-based networks for distributed training workloads. While encouraging, the silicon photonics technology is not yet commercially available, which begs the question: "Can we build an optimized network topology for DNN training clusters using today's commodity hardware?"

To answer this question, we analyze DNN training jobs from production clusters of a large-scale service provider with billions of users, which we call BIGNET for anonymity. We demonstrate that training workloads do not satisfy standard assumptions about datacenter traffic that underlie the design of Fat-tree interconnects. Specifically, we show that (*i*) the communication overhead of large DNN training jobs increases dramatically as we increase the number of workers; and (*ii*) the traffic heatmap of DNN training jobs highly depends on their parallelization strategies and AllReduce collectives.

Motivated by these observations, we propose TOPOOPT, a DNN training system that co-optimizes network topology and parallelization strategy. In this paper, we grapple with the *algorithmic* challenges of finding the best topology, such as how to navigate the large search space across computation, communication, and topology dimensions, and also with various *operational* challenges, such as which optical switching technologies match well with the traffic patterns of various DNN models.

In particular, we cast the topology and parallelization strategy co-optimization problem as an off-line alternating optimization framework. Our optimization technique *alternates* between optimizing the parallelization strategy and optimizing the network topology. It searches over the parallelization strategy space assuming a fixed topology, and feeds the traffic demand to a TOPOLOGYFINDER algorithm. The updated topology is then fed back into the parallelization strategy search algorithm. This alternating process repeats until the system converges to an optimized parallelization strategy and topology.

We demonstrate that finding an optimized network topology for DNNs with hybrid data & model parallelism is challenging because the ideal network topology needs to meet two goals simultaneously: (*i*) allocate most of the available bandwidth to AllReduce transfers; and (*ii*) ensure a small hop-count for Model Parallel transfers. To meet these goals, we propose a novel *group theory-based technique*, called TotientPerms. Our TotientPerms approach builds a series of *AllReduce permutations* that not only carry AllReduce transfers efficiently, but also are well-positioned to carry Model Parallel transfers and, hence, improve the overall training performance.

To demonstrate the feasibility of TOPOOPT, we build a 12-server testbed with NVIDIA A100 GPUs [37] and 100 Gbps NICs. Our large-scale simulations with four representative DNN models (DLRM [20], CANDLE [3], BERT [114], VGG [107]) show that TOPOOPT reduces the training iteration time by up to $3\times$ compared to a similar-cost Fat-tree. Moreover, we demonstrate that TOPOOPT is, on average, $3.4\times$ cheaper than an ideal full bisection bandwidth

Fat-tree. Finally, we evaluate the impact of reconfiguration latency on performance and argue that today's reconfigurable optical switches are too slow for large-scale DNN workloads.

TOPOOPT is the first system with entirely commodity hardware that co-optimizes topology and parallelization strategy and is currently being evaluated for deployment at BIGNET.

2 Characterizing DNN Workloads

Data parallelism. Data parallelism is a popular parallelization strategy, whereby a batch of training samples is distributed across training nodes accelerators. Each accelerator holds a replica of the DNN model and executes the forward and backpropagation steps locally. In data parallelism, all accelerators synchronize their model weights during each training iteration. This step is commonly referred to as *AllReduce* and can be performed using various techniques, such as broadcasting [121], parameter servers [81], ring-AllReduce [2, 75, 110], tree-reduce [101], or hierarchical ring-AllReduce [111, 113].

Hybrid data & model parallelism. Prior work showed that pure data parallelism may be a suboptimal strategy for large training jobs because of the increasing cost of synchronizing model parameters across accelerators [20, 72, 76, 92, 94, 106]. In BIGNET, we use a hybrid of data & model parallelism for training large DNNs, where different parts of a DNN and its dataset are processed on different accelerators in parallel. To keep each accelerator's utilization high, we use pipeline parallelism [93] together with model parallelism, where training samples across multiple iterations are processed in parallel with the partitioned model in a *pipelined* fashion. In this paper, we use model parallelism as a generic term that includes both model and pipeline parallelism.

Types of data dependencies in DNN training. Each training iteration includes two major types of *data dependencies*. Type (1) refers to *activations* and *gradients* computed during the Forward and Backpropagation steps. This data dependency is required for each input sample. Type (2) refers to synchronizing the *model weights* across accelerators through the AllReduce step once a batch of samples are processed. Depending on the parallelization strategy, these data dependencies may result in local memory accesses or cross-accelerator traffic. For instance, in a hybrid data & model parallelization strategy, both type (1) and (2) result in cross-accelerator traffic, depending on how the model is distributed across accelerators. Given that type (1) is related to model parallelism, we refer to the network traffic created by type (1) as *MP transfers*. Similarly, we refer to the network traffic created by type (2) as *AllReduce transfers*. Note that AllReduce transfers do not strictly mean data parallelism traffic since model parallelism can also create AllReduce transfers across a subset of training nodes (§3.3).[1]

---

[1] We only consider transfers related to training because our servers have dedicated NICs for storage and other non-training traffic.

(a) Number of workers   (b) Training job duration
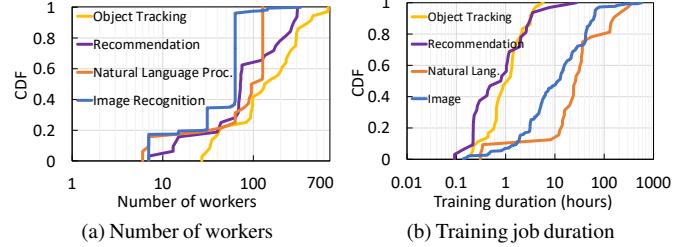
Figure 1: Profiling distributed DNN training jobs in BIGNET.

2.1 Production Measurements

We study traffic traces from hundreds of production DNN training jobs running on multiple clusters at BIGNET. We instrument each job to log its training duration, number of workers, and the total amount of data transferred across its workers during training.

Number of workers and job duration. Figure 1a shows the CDF of the number of workers for different models in our clusters. Most jobs are distributed across 32 to 700 workers, agreeing with recent announcements by other major players in the industry [43, 92]. A worker can be a CPU or a GPU depending on which cluster the job is executed on. Figure 1b demonstrates the CDF of total training job duration, showing that most jobs last over 10 hours. In fact, the top 10% of jobs take more than 96 hours (four days) to finish.

Network overhead. Figure 2 illustrates the percentage of network overhead as the number of GPUs is increased from 8 to 128 for six DNN jobs in production. We use RDMA to transmit packets between servers and measure the percentage of time consumed by communication during training as network overhead. The figure shows that as the number of GPUs increases, the network quickly takes up a significant portion of training iteration time. Similar observations have been made in prior work [56, 71, 79, 93, 105]. This is because our training servers are equipped with several NICs; hence, each server takes up several ports on its Top-of-Rack (ToR) switch, which limits the number of servers under the same rack. As a result, our network topology spans across multiple switches and racks, which, in turn, increases the likelihood of network bottlenecks.

Traffic heatmaps. Figure 3 shows the heatmap of server-to-server traffic for four training jobs running in our production GPU clusters. The rows and columns indicate source and destination servers (each with eight GPUs), while the color encodes the amount of traffic between server pairs. The values on the colormap are not shown for confidentiality reasons. All heatmaps in the figure contain diagonal squares (in dark blue), indicating a ring communication pattern between servers. This is expected since ring-AllReduce is the dominating AllReduce communication collective at BIGNET. However, the MP transfers (light blue and green squares) are *model-dependent* because MP transfers depend on the parallelization strategy and device placement of a training job. Moreover, we find that the traffic patterns of our training jobs do not change between iterations *for the entire training duration*, resulting in exactly the same heatmaps throughout the training time. Once a training
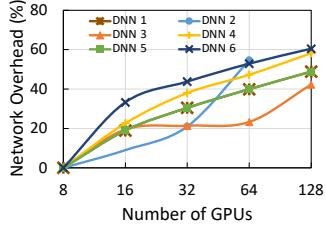
Figure 2: Network overhead measurements in BIGNET.
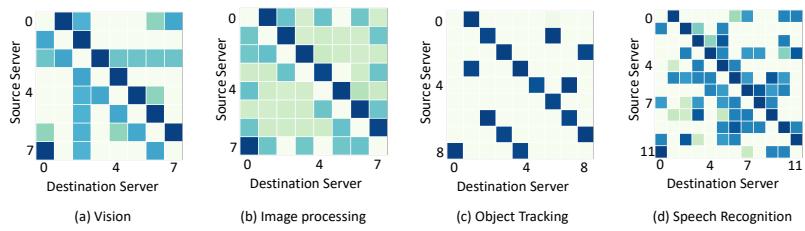
Figure 3: Traffic heatmaps of production jobs in BIGNET.
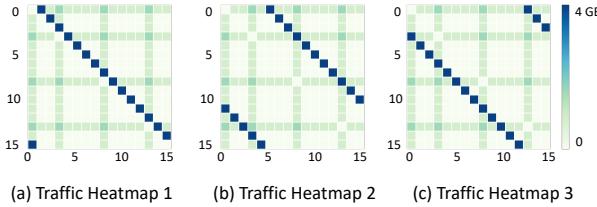
Figure 4: DLRM traffic heatmaps.
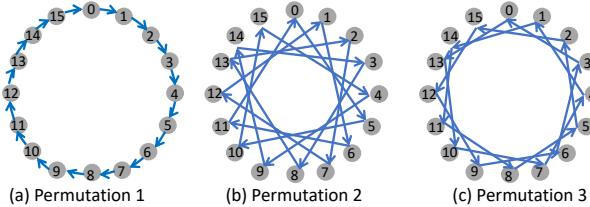
Figure 5: Ring-AllReduce permutations.
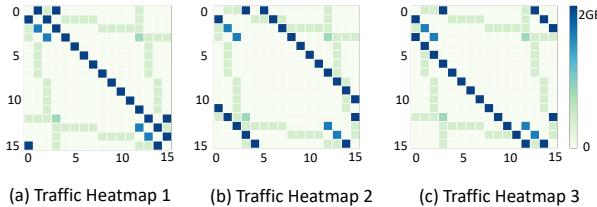
Figure 6: CANDLE traffic heatmaps.

job starts, the same parallelization strategy and synchronization method are used across training iterations, resulting in a periodic and predictable traffic pattern. Similar observations have been made in prior work [120]. In particular, the traffic heatmap is identical *between* different training iterations. Note that the traffic pattern changes *within* a training iteration. Section 5 evaluates the impact of reconfiguring the physical topology within training iterations vs. simply keeping the topology the same throughout the job.

2.2 Controlled Experiments

To better understand the impact of parallelization strategy on network traffic, we analyze the heatmap of two large DNN models, Deep Learning Recommendation Model (DLRM) and CANcer Distributed Learning Environment (CANDLE), distributed across 16 servers each with one GPU interconnected with a full bisection bandwidth Fat-tree topology.

DLRM traffic pattern.

DLRMs are a family of personalization and recommendation models based on embedding table lookups that capitalize on categorical user data [95]. Typically, DLRM models are large, up to 10s of trillion parameters, primarily due to their large embedding tables. Large embedding tables result in large AllReduce transfers. Moreover, the look-up time of embedding tables does not drop significantly as the batch sizes decrease. Hence, a common parallelization strategy for DLRMs is to use model parallelism to place each embedding table on one GPU and use data parallelism for the rest of the model [90]. Consider a simplified DLRM architecture with four embedding tables $E_0, \cdots, E_3$, each with embedding dimensions of 512 columns and 10^7 rows (total size 20 GB) distributed across 16 servers $S_0, \cdots, S_{15}$. Following the parallelization strategy used in BIGNET, we place E_0 on S_0, E_1 on S_3, E_2 on S_8, and E_3 on S_{13}, and replicate the rest of the model on all servers. This parallelization strategy creates a mix of MP and AllReduce traffic, shown in Figure 4. Each heatmap in 4a, 4b, and 4c corresponds to a different ring-AllReduce permutation, shown in Figures 5a, 5b, and 5c. Although all three heatmaps correspond to the *exact same parallelization strategy and device placement*, the blue diagonal lines appear at different parts of the heatmaps, depending on the order of servers in the ring-AllReduce permutation. However, MP transfers (green vertical and horizontal lines in each heatmap) are dictated by the parallelization strategy and device placement, and therefore remain at exactly the same spot in all three heatmaps. Hence, AllReduce transfers are permutable but MP transfers are not. We leverage this unique property of DNN training jobs in our TOPOLOGYFINDER algorithm (§3.3). Note that MP transfers in DLRM form one-to-many broadcast and many-to-one incast patterns to transfer the activation and gradients to all nodes because each server handling an embedding table needs to communicate with *all other servers*. The size of each AllReduce transfer in this example is 4 GB, whereas the size of MP transfers is 32 MB.

CANDLE traffic pattern. CANDLE is a family of DNN architectures used to predict the response of cancerous tumors to drug treatments, based on molecular features of tumor cells and drug descriptors [3, 6]. CANDLE models often contain several multilayer perceptrons (MLPs) for drug and cell features [3]. Consider a simplified CANDLE model with one drug MLP D_0 and one cell MLP C_0, each with a size of 4 GB. A common parallelization strategy is to distribute the model by

3
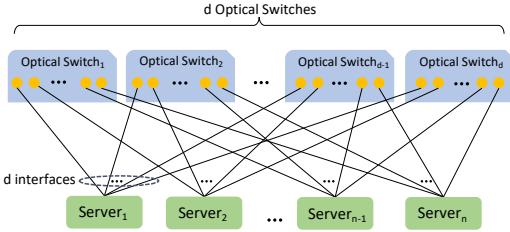
Figure 7: Illustration of TOPOOPT's interconnect.

Figure 8: TOPOOPT searches for the best parallelization strategy, jointly with routing, and topology.

replicating D_0 on four servers (e.g., $\{S_0, S_1, S_2, S_3\}$) and C_0 on another set of four servers (e.g., $\{S_{12}, S_{13}, S_{14}, S_{15}\}$). The rest of the model is replicated across all servers $\{S_0, \cdots, S_{15}\}$. This parallelization strategy creates mostly AllReduce traffic with a few MP transfers, as shown in Figure 6. Similar to the DLRM experiments, we permute the order of servers in the ring-AllReduce communication according to Figure 5 and plot three different heatmaps in Figures 6a, 6b, and 6c. Similar to the above, we confirm that the position of MP transfers remains fixed, while AllReduce transfers are permutable. We repeat the above experiment using tree-AllReduce and confirm the same takeaways hold (see Appendix A).

3 TOPOOPT System Design

This section describes TOPOOPT, a novel system based on commodity optical devices that jointly optimizes DNN parallelization strategy and topology to accelerate today's training jobs.

3.1 TOPOOPT Interconnect

A TOPOOPT cluster is a *shardable* interconnect where each server has d interfaces connected to a core layer of d optical switches, as shown in Figure 7. The optical switches enable TOPOOPT to partition the cluster dedicated partitions for each training job. The size of each partition depends on the number of servers that the job requests. Given a DNN training job and a set of servers, TOPOOPT first finds the best parallelization strategy and topology between servers off-line. Then, it reconfigures the optical switches to realize the target topology for the job.

There is a wide range of optical switching technologies suitable for a TOPOOPT cluster, including commodity available optical patch panels [41] and 3D-MEMS [16, 39], as well as futuristic designs such as Mordia [99], MegaSwitch [53], and Sirius [50, 57]. All of these technologies are valid choices for a TOPOOPT cluster. Section 4 discusses the impact of optical switching technologies on scale and reconfiguration frequency.

Degree of each server. We denote the number of interfaces on each server (i.e., the degree of the server) by d. Typically, d is the same as the number of NICs installed on the server. In cases where the number of NICs is limited, the degree can be increased with NICs that support break-out cables or with the next generation of co-packaged optical NVLinks [10]. As an example, in our testbed, we use one 100 Gbps HP NIC [29] with 4×25 Gbps interfaces to build a system with degree four
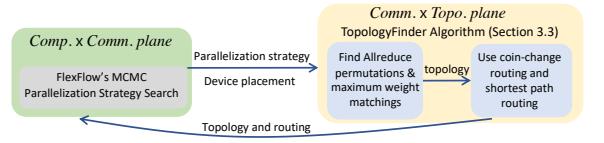
($d = 4$). Section 5 evaluates the impact of d on performance.

Target workload. The target workload for TOPOOPT is long-lasting DNN training jobs with hybrid data & model parallelism. Hence, we assume the set of servers assigned to each job remains the same throughout the lifetime of the job, and the GPUs are not shared across multiple jobs. Section 7 discusses potential approaches to enable dynamic scheduling and multi-tenancy in TOPOOPT.

Storage and control plane traffic. BIGNET's training clusters consist of custom-designed servers, each with eight GPUs, eight dedicated NICs for training traffic (GPU NICs), and four additional NICs for storage and other traffic (CPU NICs). Other companies, such as Facebook and NVIDIA, have similar server architectures [9, 90]. TOPOOPT only considers GPU NICs as server degree and partitions the network that is dedicated for training traffic. The CPU NICs are connected through a separate fabric to carry storage and other control plane traffic.

3.2 Co-optimizing Parallelization Strategy and Network Topology

The search space is too large. Finding the optimal parallelization strategy is an NP-complete problem, and adding network topology and routing makes the problem even harder [76]. An extreme solution is to jointly optimize compute, communication, and topology dimensions using a *cross-layer optimization formulation*. Theoretically, this approach can find the optimal solution, but the search space quickly explodes, even for modest networks (e.g., six nodes [109]). Our cross-layer optimization problem is computationally expensive, as it needs to evaluate a large number of operator placements and network configurations.

Naive approach. The other extreme is to optimize the network topology *sequentially after* the parallelization strategy has been found. While this approach is able to reconfigure the network to better match its traffic demand, the eventual combination of topology and parallelization strategy may be sub-optimal in the global configuration space because the parallelization strategy search algorithm needs to assume a generic static network topology and might miss opportunities to find a better strategy enabled by a different topology.

Our approach: alternating optimization. In TOPOOPT, we seek to achieve the best of both worlds. To make the problem tractable, we divide the search space into two planes: *Comp.* × *Comm.* and *Comm.* × *Topo.* and use an alternating optimization technique to iteratively search in one plane while keeping the result of the other plane constant. Figure 8 illustrates TOPOOPT's alternating optimization framework. The

green box represents our *Comp.×Comm.* plane, which uses FlexFlow's MCMC (Markov Chain Monte Carlo) search algorithm [76] to find the best parallelization strategy for a given topology while considering the link bandwidths as communication cost. We feed the output of FlexFlow's parallelization strategy to our *Comm.×Topo.* plane each time it finds a strategy with improved runtime, or after 50 iterations of MCMC search when it cannot find an improvement, to escape local optimums. The yellow box in Figure 8 represents TOPOOPT's *Comm.×Topo.* plane where, given a parallelization strategy and device placement as input, it finds the best network topology and routing to minimize the training iteration time using our TOPOLOGYFINDER algorithm. The best discovered topology is fed back into the *Comp.×Comm.* plane, which further optimizes the parallelization strategy and device placement based on the updated topology. This optimization loop repeats until convergence or after *k* iterations, where *k* is a configurable hyper-parameter. The next subsection describes our TOPOLOGYFINDER algorithm inside the *Comm.×Topo.* plane.

3.3 TOPOLOGYFINDER Algorithm

Prior proposals are inefficient for DNN workloads. At first blush, finding a network topology seems straightforward: we just need to translate the parallelization strategy and device placement from *Comp.×Comm.* plane into a traffic matrix and map the traffic matrix into circuit schedules. Several prior papers have addressed this problem for datacenter networks [53, 60, 64, 68, 79, 83–85, 99, 117]. The conventional wisdom in prior work is to allocate as many direct parallel links as possible to *elephant flows* and leaves *mice flows* to take multiple hops across the network. In principle, this approach works well for datacenters but we argue it leads to sub-optimal topologies for distributed DNN training because the size of AllReduce transfers is larger than MP transfers in BIGNET (Appendix B). Hence, the conventional approach leads to creating parallel direct links for carrying AllReduce traffic and forcing MP flows to have a large hop-count. But MP transfers are on the critical path of processing every batch, and a slight delay in their completion time negatively impacts the entire training iteration time. Consequently, having a large hop-count for MP transfers degrades training performance.

TOPOOPT's novel technique. In TOPOOPT, we seek to meet two goals simultaneously: (*i*) allocate most of the available bandwidth to AllReduce transfers since the bulk of the traffic belongs to them; but (*ii*) ensure a small hop-count for MP transfers. We meet both goals by leveraging a unique property of distributed DNN training traffic, namely that the AllReduce part of the traffic matrix is *mutable* and can be split across multiple permutations (§2.2). Intuitively, this is because MP traffic is composed of network flows among nodes that contain *different* parts of a DNN model thus creating immutable data dependencies across these nodes, while AllReduce transfers contain network flows among nodes that handle the *same* part of the model, providing flexibility on the order of nodes par-

ticipating in AllReduce. Consequently, if a group of servers is connected in a certain order, simply permuting the labeling of the servers gives another ordering that would finish the AllReduce operation with the same latency while potentially providing a smaller hop-count for MP transfers. Instead of selecting just one AllReduce order, we find multiple permutations for each AllReduce group that best satisfy MP transfers and overlap their corresponding sub-topologies. In doing so we, not only serve the AllReduce traffic, but also decrease the hop-count for MP transfers.

TOPOLOGYFINDER steps. Algorithm 1 presents the pseudocode of our TOPOLOGYFINDER algorithm. The algorithm takes the following inputs: *N* dedicated servers for the training job, each with degree *d*, as well a list of AllReduce and MP transfers ($T_{AllReduce}$ and T_{MP}) based on the parallelization strategy and device placement obtained from the *Comp.×Comm.* plane. The algorithm then finds the best topology (*G*) and routing rules (*R*) and returns them to the *Comp.×Comm.* plane for the next round of alternating optimization. Our algorithm consists of the following four steps.

Step 1: Distribute the degree. The first step distributes the degree *d* between AllReduce and MP sub-topologies proportionally, based on their share of total traffic. We specifically start with AllReduce transfers and allocate at least one degree to the AllReduce sub-topology to ensure the network topology remains connected (line 2). The remaining degrees, if any, are allocated to the MP sub-topology (line 3).

Step 2: Construct the AllReduce sub-topology and routing. To find the AllReduce sub-topology, the algorithm iterates over every AllReduce group *k* and allocates degree d_k to each group proportionally based on the amount of traffic they require (line 6). Note that in hybrid data & model parallelism strategies, the AllReduce step can be performed across a subset of servers when an operator is replicated across a few servers instead of all servers. For each AllReduce group *k*, TOPOLOGYFINDER efficiently finds a set of permutations across those servers in *k* (line 8). It then selects the top d_k permutations that *best satisfy MP traffic demands* using a module called `TopPermutations` (line 9). There are several metrics to use in `TopPermutations` module to measure satisfaction of MP demand. In our implementation, we use the sum of MP transfer sizes with a *direct link from AllReduce permutations* as our metric. TOPOLOGYFINDER's approach of selecting AllReduce permutations while considering MP traffic demand is a key reason to look for alternative AllReduce permutations. However, at large scales, finding the set of all possible AllReduce permutations is non-trivial, since the number of possible permutations is $O(n!)$, where *n* is the number of servers in group *k*. Inspired by group theory, we develop a technique to address this challenge, called TotientPerms, described next.

Using group theory to find AllReduce permutations. Given that ring-AllReduce is the dominant AllReduce collective in BIGNET, we describe our `TotientPerms` technique based on ring-AllReduce. Appendix C explains how to ex-

Algorithm 1 TOPOLOGYFINDER pseudocode

1: **procedure** TOPOLOGYFINDER(N, d, $T_{AllReduce}$, T_{MP})
   ▷ **Input** N: Number of dedicated training servers for the job.
   ▷ **Input** d: Degree of each server.
   ▷ **Input** $T_{AllReduce}$: AllReduce transfers.
   ▷ **Input** T_{MP}: MP transfers.
   ▷ **Output** G: Topology to give back to the $Comp. \times Comm.$ plane.
   ▷ **Output** R: Routing rules to give back to the $Comp. \times Comm.$ plane.
   ▷ *Distribute degree d between AllReduce and MP sub-topologies*
2:    $d_{AllReduce} = \max(1, \lceil d \times \frac{sum(T_{reduce})}{sum(T_{reduce}) + sum(T_{MP})} \rceil)$
3:    $d_{MP} = d - d_{AllReduce}$
     ▷ *Construct the AllReduce sub-topology $G_{AllReduce}$*
4:    $G_{AllReduce} = \{\}$
5:    **for** each AllReduce group k with set of transfers T_k **do**
       ▷ *Assign degree d_k to group k according to its total traffic*
6:       $d_k = \lceil d_{AllReduce} \times \frac{sum(T_k)}{sum(T_{reduce})} \rceil$
7:       $d_{AllReduce} = d_{AllReduce} - d_k$
       ▷ *Find all the permutations between servers in group k*
8:       $P_k = \texttt{TotientPerms}(N, k)$
       ▷ *Select d_k permutations from P_k according to T_{MP}*
9:       $G_{AllReduce} = G_{AllReduce} \cup \texttt{TopPermutations}(N, d_k, P_k, T_{MP})$
10:      **if** $d_{AllReduce} == 0$ **then**
11:        break
    ▷ *Compute routes on $G_{AllReduce}$ using the coin change algorithm [49]*
12:   $R = \texttt{CoinChangeMod}(N, G)$
    ▷ *Construct the MP sub-topology G_{MP}*
13:   $G_{MP} = \{\}$
14:   **for** $i : i < d_{MP}$ **do**
      ▷ *Find a maximum weight matching according to T_{MP}*
15:      $g = \texttt{BlossomMaximumWeightMatching}(T_{MP})$
16:      $G_{MP} = G_{MP} \cup g$
      ▷ *Reduce the amount of demand for each link l in graph g*
17:      **for** $l \in g$ **do**
18:        $T_{MP}[l] = T_{MP}[l] / 2$
    ▷ *Combine the AllReduce and MP topologies*
19:   $G = G_{AllReduce} \cup G_{MP}$
    ▷ *Compute routes on G_{MP} with shortest path*
20:   $R += \texttt{ShortestPath}(G, T_{MP})$

(a) TOPOOPT topology   (b) TOPOOPT traffic pattern

Figure 9: Example of TOPOOPT's topology and traffic matrix.

In classical coin change, the goal is to find the minimum number of *coins* that would sum to a certain *total value*. Our ring generation rules enable us to treat the routing problem similarly. In particular, the p values of AllReduce permutations that have been selected in the AllReduce sub-topology are the coin values, and the difference between server i and j indices $((j-i) mod n)$ is the target total value that we want to achieve. The only difference is that our problem runs in *modulo n* arithmetic space, as the server IDs wrap around in the ring structure. Appendix C lists the pseudocode of TotientPerms, TopPermutations, and CoinChangeMod methods.

Step 3: Construct the MP topology. Given that MP transfers are not permutable, we use the classical Blossom maximum weight matching algorithm [59] to find the best connectivity between servers with MP transfers (line 15). We repeat the matching algorithm until we run out of degrees. To increase the likelihood of more diverse connectivity across server pairs, we divide the magnitude of T_{MP} for pairs that already have an edge between them by two (line 18). In general, division by two can be replaced by a more sophisticated function with a diminishing return. Appendix D elaborates on this point.

Step 4: Final topology and routing. Finally, we combine the MP and AllReduce sub-topologies and compute k-shortest path routes for MP transfers (lines 19 and 20).

Example. We use the DLRM model in Figure 4 distributed across 16 servers each with six NICs ($d = 6$) as an example. Instead of choosing one of the AllReduce permutations in Figure 5, TOPOOPT combines the three ring-AllReduce permutations to load-balance the AllReduce transfers while providing a short hop-count for MP transfers. Figure 9 illustrates TOPOOPT's topology and traffic matrix, demonstrating a more balanced traffic matrix than Figure 4.

4 Optical Switching Technologies

Once an optimized topology and parallelization strategy is found for a given job, we use optical switches in TOPOOPT to reconfigure the interconnection between the set of servers that participate in the job. Since our TOPOLOGYFINDER algorithm takes the server degree d as input, we directly map the output of the algorithm to a physical topology.

There are many different optical switching technologies that we can use for TOPOOPT [41, 50, 53, 54, 57, 60, 64, 79, 83, 85, 87, 88, 99, 104]. Table 1 lists the key characteristics of these technologies. In principle, TOPOOPT's design is compatible

tend our algorithm to other AllReduce communication collectives. For a ring-AllReduce group with n servers labeled $S_0, ..., S_{n-1}$, a straightforward ring-AllReduce permutation is $(S_0 \rightarrow S_1 \rightarrow S_2 \cdots \rightarrow S_{n-1} \rightarrow S_0)$. We denote this permutation by a ring generation rule as: $S_i \rightarrow S_{(i+1) \ mod \ n}$. Since the servers form a ring, the index of the starting server does not matter. For instance, these two rings are equivalent: $(S_0 \rightarrow S_1 \rightarrow S_2 \rightarrow S_3 \rightarrow S_0)$ and $(S_1 \rightarrow S_2 \rightarrow S_3 \rightarrow S_0 \rightarrow S_1)$. To reduce the search space of all possible permutations, we find the ring generation rule for all *regular rings*; i.e., rings where the distance between indices of consecutive servers is equal; i.e., server S_i is connected to server $S_{(i+p) \ mod \ n}$. In particular, we show that all integer numbers $p < n$, where p is co-prime with n (i.e. $gcd(p,n) = 1$), represent a valid ring-AllReduce permutation (Appendix C). For instance, for $n = 12$ servers, our ring generation rule with $p = 1, 5, 7, 11$ will lead into 4 distinct AllReduce permutations between the servers. In cases where n is extremely large, we restrict p to prime numbers, thus reducing the search space to only $\frac{n}{\ln n}$ according to the Prime Number Theorem [62]. The eventual AllReduce sub-topology is the union of top permutations selected in line 9.

Coin-change routing. Consider servers S_i and S_j that need to exchange AllReduce transfers but do not have a direct edge between them. We use a modified version of the classical coin change problem [49] to find an efficient routing path (line 12).

Technology	Port-count	Reconfig. latency	Insertion Loss (dB)	Cost /port
Optical Patch Panels [41]	1008	minutes	0.5	$100
3D MEMS [16, 39]	384	10 ms	1.5–2.7	$520
2D MEMS [53, 99]	300	11.5 μs	10–20	Not commercial
Silicon Photonics [79, 104]	256	900 ns	3.7	Not commercial
Tunable Lasers [50, 57]	128	3.8 ns	7-13	Not commercial
RotorNet [87, 88]	64	10 μs	2	Not commercial

Table 1: Comparison of optical switching technologies.

with any of these technologies. However, most are not commercially available. For an immediate deployment in BIGNET, this section focuses on optical patch panels [41, 102] and 3D MEMS circuit switches [16, 39], the only two technologies that are commercially available today. In our simulations, we evaluate the performance of fast reconfigurable switches to provide a perspective on future designs (§5).

Optical patch panels. Fiber optic patch panels are commonly used for cable management. Reconfigurable optical patch panels are a new class of software-controlled patch panels and are already commercialized at scale [102]. For instance, Telescent offers fully reconfigurable patch panels with 1008 duplex ports and insertion loss less than 0.5 dB for $100K ($100/port) [41, 102]. Reconfiguration is performed using a robotic arm that grabs a fiber on the transmit side and connects it to a fiber on the receive side [78]. However, the reconfiguration latency of optical patch panels is several minutes [41].

3D MEMS-based Optical Circuit Switches (OCSs). An OCS uses tiny mirrors to change the direction of light, thereby reconfiguring optical links. The largest optical circuit switch on the market has 384 duplex ports with ≈10 ms reconfiguration latency and is available for $200K ($520/port) [39]. However, the optical loss of these switches is 1.5–2.7 dB [19]. Compared to patch panels, OCSs have the following disadvantages: (*i*) each port is five times more expensive; (*ii*) their insertion loss is higher; and (*iii*) their port-count is three times lower. The main advantage of OCSs is that their reconfiguration latency is *four orders of magnitude* faster than patch panels.

Impact of reconfiguration latency. Patch panel and OCS technologies are both applicable to TOPOOPT. The choice of which technology to use depends on several factors, including scale of the cluster, iteration training time of jobs, and frequency of job arrivals. For instance, OCSs can be used to reconfigure the topology of a job *within* training iterations, whereas patch panels are only suitable when the topology remains intact throughout the entire training. Our evaluations demonstrate that the reconfiguration latency of today's OCSs is too high for some DNNs, leading to sub-optimal performance when the topology is reconfigured within iterations (§5).

Handling job arrivals. To start a job with k servers, we need to reconfigure the interconnection between these k servers before the job starts. This can be done quickly when OCSs are used, but when patch panels are used, there could be several minutes of delay before the job can start. To address this challenge, we use a look-ahead approach to pre-provision the next topology while current jobs are running. More specifically,
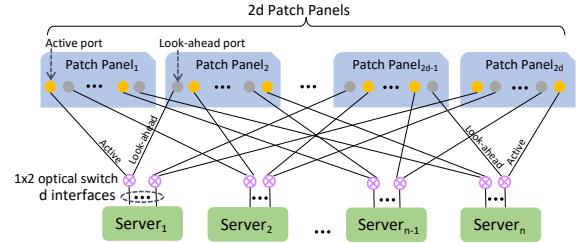
Figure 10: Active & Look-ahead ports when the reconfiguration latency is too high.

we use a simple 1×2 mechanical optical switch [98] at each server's interface to choose between *Active* vs. *Look-ahead* ports. These 1×2 switches are inexpensive ($25) and have 0.73 dB optical loss measured in our prototype. We then connect the two ends of each 1×2 switch to different patch panels, as shown in Figure 10. As a result, a TOPOOPT cluster with n servers, each with d interfaces, has $2d$ patch panels where each interface is split into two parts: Active and Look-ahead. At any point in time, only one end of each 1×2 switch is participating in the active topology; the other end is pre-provisioning the topology for the next job. Once all the servers for the new job are ready, TOPOOPT immediately *flips* to the new topology by reconfiguring the corresponding 1×2 switches.

5 Large-Scale Simulations

This section evaluates the performance of a large-scale TOPOOPT interconnect. First, we explain our simulation software and methodology (§5.1). Then, we provide a cost analysis of TOPOOPT to inform our simulations when comparing different interconnects (§5.2). Next, we demonstrate the performance of TOPOOPT when a cluster is dedicated to a single distributed DNN training job (§5.3). We extend this setting to a case where a training cluster is shared among multiple DNNs (§5.4). Finally, we demonstrate the impact of reconfiguration latency and server degree on TOPOOPT's performance (§5.5).

5.1 Methodology & Setup

We implement two simulators to evaluate TOPOOPT:

FlexNet **simulator.** We augment FlexFlow's simulator [27] to be network-aware and call it *FlexNet*. Given a DNN model architecture and a batch size, FlexFlow's simulator explores different parallelization strategies and device placements to find a strategy that minimizes per-iteration training time. The output of the FlexFlow simulator is a *task graph* describing the set of computation and communication tasks on each GPU and their dependencies. However, current implementation of FlexFlow ignores the network topology entirely by assuming servers are connected in a *full-mesh* interconnect. Our *FlexNet* simulator extends the FlexFlow simulator and enables it to consider multiple networks, including Fat-trees, TOPOOPT, and expander networks. Moreover, *FlexNet* implements our alternating optimization framework (§3) to find an optimized network topology and routing rules for TOPOOPT.

	VGG	BERT	DLRM	CANDLE
Batch size/GPU: 64	Batch size/GPU: 16 #Trans. blks: 12 Hidden layer: 1024 Seq. length: 64 #Attn. heads: 16 Embed. size: 512	Batch size/GPU: 128 #Dense layer: 8 Dense layer size: 2048 #Dense feat. layer: 16 Feat. layer size: 4096 Embed.: 128×10^7 #Embed. tables: 64	Batch size/GPU: 256 #Dense layer: 8 Dense layer: 16384 #Dense feat. layer: 16 Feat. layer size: 16384
Batch size/GPU: 64	Batch size/GPU: 16 #Trans. blks: 6 Hidden layer: 768 Seq. length: 256 #Attn. heads: 6 Embed. size: 512	Batch size/GPU: 256 #Dense layer: 8 Dense layer size: 1024 #Dense feat. layer: 16 Feat. layer size: 2048 Embed.: 256×10^7 #Embed. tables: 16	Batch size/GPU: 256 #Dense layer: 8 Dense layer: 4096 #Dense feat. layer: 16 Feat. layer size: 4096

Table 2: DNN models used in our simulations.

Link band-width	Transceiver ($)	NIC ($)	Electrical switch port ($)	Patch panel port ($)	OCS port ($)	1×2 switch ($)
10 Gbps	20 [12]	180 [32]	87 [21]	100 [41]	520 [39]	25 [98]
25 Gbps	39 [13]	185 [33]	144 [23]	100 [41]	520 [39]	25 [98]
40 Gbps	39 [14]	376 [17]	144 [22]	100 [41]	520 [39]	25 [98]
100 Gbps	99 [11]	660 [34]	225 [24]	100 [41]	520 [39]	25 [98]
200 Gbps[2]	198 [11]	790 [35]	450 [24]	100 [41]	520 [39]	25 [98]

Table 3: Cost of network components.

Figure 11: Interconnect cost comparison.

FlexNetPacket simulator. We find that FlexFlow's simulator often underestimates the training iteration time at large scales because it does not simulate packets traversing through a network. Extending *FlexNet* to become a packet-level simulator is not computationally feasible, since FlexFlow generally requires thousands of MCMC rounds to converge. To faithfully simulate per-packet behavior of network switches, buffers, and multiple jobs sharing the same fabric, we build a second event-based packet simulator, called *FlexNetPacket*, on top of htsim [5]. *FlexNetPacket* takes the output of *FlexNet*– that is, the optimized parallelization strategy, device placement of each operator, optimized network topology, and routing rules – and simulates several training iterations. The simulated training iterating times with *FlexNetPacket* match those we observe in BIGNET's clusters. The per-hop latency in *FlexNetPacket* is set to 1 μs to reflect the multi-hop latency of servers that are not directly connected. These two simulators together are $\approx$10K lines of code in C++. We will release our codebase and all related data and scripts online.

Simulated network architectures. We simulate distributed training clusters with n servers equipped with four NVIDIA A100 GPUs [37]. We vary n in different experiments and simulate the following network architectures:

• **TOPOOPT-oneshot.** A TOPOOPT interconnect where each server is equipped with d NICs, each with bandwidth B connected via a flat layer of optical devices. At the beginning of each job, the topology is reconfigured based on the output of our alternating optimization framework (§3) and remains unchanged throughout the entire training job. Both OCS and patch panels are suitable for this architecture.

• **TOPOOPT-reconfig.** To study the impact of changing the network topology within training iterations, we simulate a reconfigurable TOPOOPT interconnect. We only rely on OCSs for this design and assume their reconfiguration latency is 10 ms. Given that FlexFlow's parallelization strategy search is not aware of dynamically reconfigurable networks, following prior work [79], we measure the traffic demand every 50 ms and adjust the circuits based on a heuristic algorithm to satisfy the current traffic demand as much as possible (Appendix D).

• **Ideal Fat-tree.** An ideal full bisection bandwidth Fat-tree where each server has one NIC and the bandwidth of every link is $d \times B$. This architecture provides an ideal bound for training iteration times in a cluster where each server has $d \times B$ available network bandwidth.

• **Cost-equivalent Fat-tree.** To compare the performance of TOPOOPT with a cost-equivalent architecture, we simulate a full bisection bandwidth Fat-tree where each server has one NIC and the bandwidth of each link is $d \times B'$, where B' is lower than B and is selected such that this Fat-tree has a similar cost to TOPOOPT (§5.2).

• **Oversub. Fat-tree.** This is a 2:1 oversubscribed Fat-tree interconnect, similar to the one used in Opera [87], where the bandwidth of each link is $d \times B$ but half of the links at the ToR uplink layer are omitted.

• **SiP-ML [79].** SiP-ML is a futuristic DNN training cluster with several Tbps bandwidth per GPU. While having a Tbps network is certainly a plus, our goal is to compare the algorithmic contributions of TOPOOPT and SiP-ML. Hence, to make an apples-with-apples comparison, we allocate d wavelengths, each with bandwidth B, to each SiP-ML GPU and follow its SiP-Ring algorithm to find a topology with a reconfiguration latency of 25 μs. Appendix E elaborates on our modifications to SiP-ML.

• **Expander [108, 115].** Finally, we simulate a fabric where each server has d NICs with bandwidth B interconnected via an Expander topology.

DNN Workloads. We simulate four real-world DNN models: DLRM [20], CANDLE [3], BERT [58], and VGG [107]. Table 2 summarizes model configurations and batch sizes used in our simulations. The top and bottom rows correspond to models used in Sections 5.3 and 5.4, respectively. Batch sizes are selected based on the common batch sizes used in BIGNET. Each data point averages 5–20 simulation runs.

Parallelization strategy. We use *FlexNet*'s topology-aware parallelization strategy search for Ideal Fat-tree, Cost-equivalent Fat-tree, Oversub. Fat-tree, SiP-ML, and Expander

---

[2] 200 G transceivers and switch ports are estimated as 2× 100G cost.
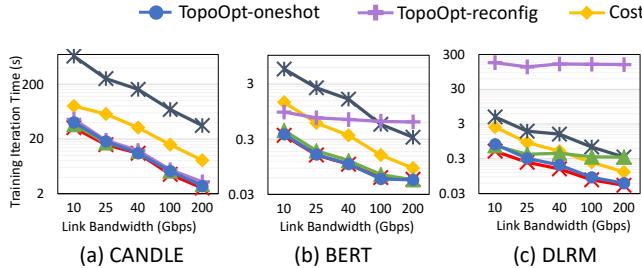
Figure 12: Dedicated cluster of 128 servers ($d = 4$).

Figure 13: Dedicated cluster of 128 servers ($d = 8$).

networks. For TOPOOPT, we use *FlexNet*'s alternating optimization framework to find the best parallelization strategy jointly with topology. We use ring-AllReduce and distributed parameter server [81] as default AllReduce communication collectives between servers and within servers, respectively.

5.2 Cost Analysis

We begin our evaluations by comparing the cost of different network architectures. Table 3 lists the cost of network components we use in this section. The cost of transceivers, NICs, and electrical switch ports is based on the lowest available prices in official retailer websites. We obtain the cost of patch panel, OCS, and 1×2 optical switch directly from their suppliers. Note that the cost of optical components stays constant as link bandwidth increases, an inherent advantage of optics. Following prior work, we estimate the cost of fiber optics cables as 30 cents per meter [64] and select each fiber's length from a uniform distribution between 0 and 1000 meters [126].

Figure 11 compares the interconnect cost across various network architectures as the number of servers is increased. We calculate the cost of TOPOOPT-oneshot based on $2d$ patch panels and 1×2 switches at each link to support its look-ahead design (§4). TOPOOPT-reconfig's cost is based on d OCSs connected to all servers in a flat topology. We make the following observations. First, using OCSs for TOPOOPT is more expensive ($1.33 \times$, on average) than patch panels. Note that OCSs can be used in both TOPOOPT-oneshot and TOPOOPT-reconfig interconnects. Second, the cost of TOPOOPT-oneshot (blue curve) overlaps with the Cost-equivalent Fat-tree (yellow curve). This is intentional, since having a cost-equivalent architecture enables us to compare the performance of TOPOOPT to a cluster at the same price point. Third, TOPOOPT-oneshot is, on average, $3.4 \times$ more cost effective than its Ideal Fat-tree counterpart. Finally, the most and least expensive fabrics are SiP-ML and Expander, respectively, and this section shows that they both perform worse than TOPOOPT.

We acknowledge that estimating the cost of networking hardware is challenging because prices are subject to significant discounts with bulk orders. However, assuming all components in this analysis are subject to the same bulk order discounts, the relative comparison across architectures remains valid.
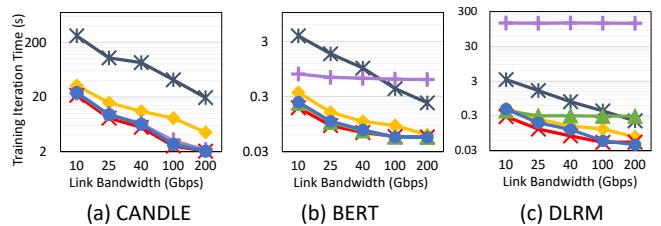
5.3 Performance Comparison for Dedicated Clusters

Figure 12a demonstrates the training iteration time of CANDLE distributed on a dedicated cluster of 128 servers with four A100 GPUs where $d = 4$. We vary the link bandwidth (B) on the x-axis. There are three takeaway points from this figure. First, Ideal Fat-tree, TOPOOPT-oneshot, TOPOOPT-reconfig, and SiP-ML architectures all achieve similar performance for CANDLE. This is because the best parallelization strategy for CANDLE at this scale is mostly data parallel, with a few MP transfers, hence the network topology matters less. Recall that TOPOOPT-oneshot has the lowest cost across these architectures. Second, the Cost-equivalent Fat-tree architecture has, on average, $2.8 \times$ higher training iteration time than these four architectures. Third, the Expander architecture has the worst performance, since it is not optimized for DNN workloads.[3,4]

The difference between those overlapping architectures starts to matter for BERT, shown in Figure 12b. In particular, this time, only three architectures overlap: TOPOOPT-oneshot, Ideal Fat-tree, and SiP-ML because BERT's parallelization strategy includes more MP transfers than CANDLE; hence, the impact of network topology on training iteration time is more pronounced. As a result, TOPOOPT-reconfig's performance starts to suffer since the reconfiguration latency of OCSs is long compared to the training iteration time of BERT at this scale.

DLRM's case is even more interesting, as it has a lot more MP transfers than the other two DNNs. As shown in Figure 12c, TOPOOPT-oneshot's performance remains close to the Ideal Fat-tree but both SiP-ML and TOPOOPT-reconfig perform poorly and despite increasing the link bandwidth, their training iteration time stays flat. This happens because DLRM has a lot of one-to-many and many-to-one broadcast and incast MP transfers which require several circuit reconfigurations to meet the traffic demand, consequently hurting the performance of both SiP-ML and TOPOOPT-reconfig. In particular, TOPOOPT-reconfig is performing two orders of magnitude worse than SiP-ML because its reconfiguration latency is two orders of magnitude higher (10 ms vs. 25 μs). To verify this conclusion, we run a series of simulations without reconfiguring TOPOOPT-reconfig and SiP-ML and observe that their performance

---

[3]We note that it might be possible to improve the performance of the Expander fabric by augmenting Blink's approach [116] to a cluster-level solution.

[4]VGG's results are similar to CANDLE (figures omitted).
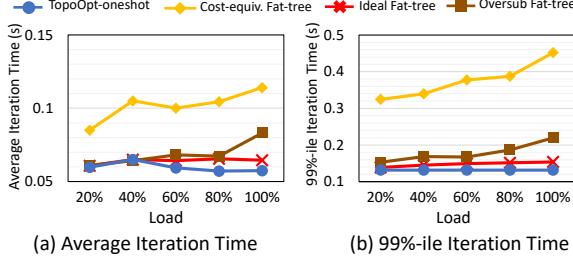
Figure 14: Shared cluster of 432 servers ($d = 8$, $B = 100$ Gbps).

Figure 15: Impact of reconfiguration latency.

Figure 16: Impact of server degree (d) on performance.

matches TOPOOPT-oneshot. Section 5.5 evaluates the impact of reconfiguration latency on performance and shows that we need optical switches with faster reconfiguration latency, such as Sirius [50], to meet the performance of Ideal Fat-tree.

Figure 13 shows the same setting as Figure 12 except that each server now has eight NICs. The results show a similar trend: even though per server bandwidth has increased, the behavior of different network architectures remains consistent. In summary, across all data points in Figures 12 and 13, TOPOOPT-oneshot has $2.2\times$ better training iteration time than its Cost-equivalent Fat-tree counterpart.

5.4 Performance Comparison for Shared Clusters

We now compare the performance of different network architectures when the cluster is shared across multiple DNN jobs. Following prior work [86, 100], we run a series of simulations where 40% of the jobs are DLRM, 30% are BERT, 20% are CANDLE, and 10% are VGG16. We change the number of active jobs to represent the load on the cluster.

Figure 14 compares the average and 99%-tile iteration time at different loads for a cluster with 432 servers, where $d = 8$ and $B = 100$ Gbps. SiP-ML does not support multiple jobs, hence we omit it in this experiment. Moreover, we omit TOPOOPT-reconfig and Expander networks since they both have a poor performance in this setting. Instead, we add the Oversub. Fat-tree interconnect to demonstrate the impact of congestion on Fat-tree topologies. Figure 14a shows that TOPOOPT-oneshot improves the average iteration time by $1.7\times$ and $1.16\times$, compared to Cost-equivalent Fat-tree and Oversub. Fat-tree architectures, respectively. Moreover, TOPOOPT improves the training time of Ideal Fat-tree fabric by $1.07\times$ on average! Initially, we were surprised by this result since we expected Ideal Fat-tree would have the lowest possible iteration time. However, we find two reasons why TOPOOPT out-performs Ideal Fat-tree: (*i*) the workload consists of large incast transfers causing congestion in the network that Fat-tree interconnects are notoriously vulnerable to, and (*ii*) TOPOOPT provides better latency properties, as most servers are at most three hops away, whereas for Fat-trees, the maximum hop count is six. We observe a similar trend for the tail iteration completion times, depicted in Figure 14b. Averaging across all load values on the x-axis, TOPOOPT improves the tail training iteration time by $3\times$, $1.4\times$, and $1.12\times$, compared to Cost-equivalent Fat-tree,
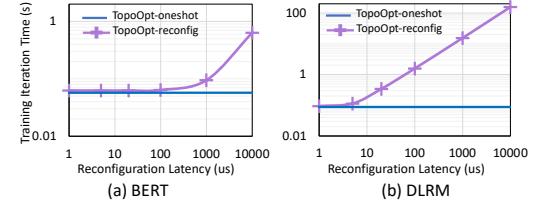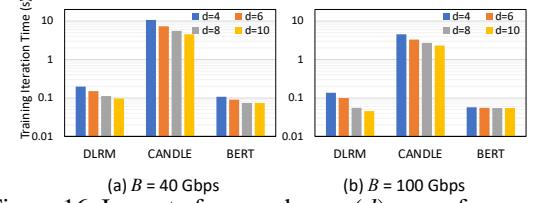
Oversub. Fat-tree, and Ideal Fat-tree architectures, respectively.

5.5 Sensitivity Analysis

Impact of reconfiguration latency. The results presented in Figures 12 and 13 indicate that reconfiguring the topology within training iterations can lead to poor performance in some cases. One way to address this issue is to keep the topology the same throughout the entire training time (similar to our TOPOOPT-oneshot design). While our experiments show that keeping the topology intact achieves training iteration time as good as the Ideal Fat-tree fabric most of the time, intellectually, it is important to understand whether there is a suitable reconfiguration latency for DNN training clusters. Figure 15 shows the training iteration time of BERT and DLRM in the same setting as in Figure 12 while sweeping the reconfiguration latency of OCSs in TOPOOPT-reconfig from 1 μs to 10 ms. The horizontal blue line corresponds to TOPOOPT-oneshot's iteration time which remains constant as it does not reconfigure the network topology. The figure shows that when the reconfiguration latency is lower than 1 μs, the iteration time of TOPOOPT-reconfig matches that of TOPOOPT-oneshot. Fast reconfigurable switches are going to be essential in elastic scenarios where the cluster is shared across multiple jobs and servers join and leave different jobs unexpectedly. This is a challenging research problem, and we leave the design of a joint topology optimization, cluster scheduling, and parallelization strategy to future work. We believe futuristic fast reconfigurable switches, such as Sirius [50], are well-suited for this setting but finding a parallelization algorithm that is aware of reconfigurability in the network topology is a challenging and exciting future research problem.

Impact of server degree. We next study the impact of server degree d on TOPOOPT's performance. Specifically, we vary the degree of each server in TOPOOPT for two link bandwidths: 40 Gbps and 100 Gbps. Figure 16 shows the trend for different DNN models. Both DLRM and CANDLE are network-heavy; therefore, they benefit more from the additional bandwidth obtained by increasing d. CANDLE's improvement is almost linear as degree goes up, as the strategy is closer to data parallel
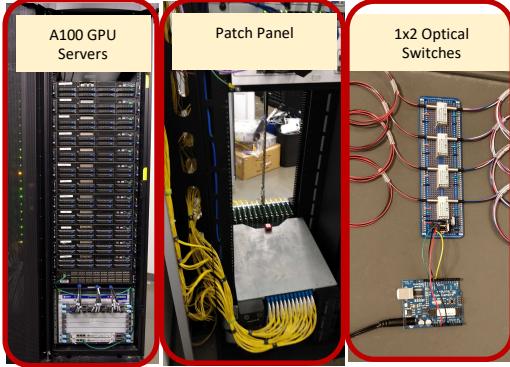
Figure 17: Photo of our testbed.

ResNet50	BERT	CANDLE
Batch size/GPU: 20 dataset: CIFAR10	Batch size/GPU: 2 #Trans. blks: 4 Hidden layer sz: 768 Seq. length: 64 #Attn. heads: 16 Embed. size: 512	Batch size/GPU: 10 #Dense layer: 4 Dense layer sz: 4096 #Dense feat. layer: 8 Feat. layer size: 4096

Table 4: DNN models used in our testbed.

Figure 18: Training through-put (samples/second).

Figure 19: Time-to-accuracy of ResNet50.

and the amount of bandwidth available to AllReduce operation increases linearly as well. In the case of DLRM, we observe a super-liner scaling when $B = 100$ Gbps. This is because DLRM has one-to-many and many-to-one MP transfers which require a low hop count in the topology. As we increase d, TOPOLOGYFINDER is able to find network topologies with much lower diameter, consequently benefiting the performance by both increasing bandwidth and reducing hop-count for MP transfers. Finally, BERT is mostly compute bound at higher bandwidth; hence, increasing the server degree and bandwidth per node has marginal impact on its iteration time.

6 Prototype

Testbed setup. We build a prototype to demonstrate the feasibility of TOPOOPT. Our prototype includes 12 ASUS ESC4000A-E10 servers and a G4 NMT patch panel [41]. Each server is equipped with one A100 Nvidia GPU [37] (40 GB of HBM2 memory), one 100 Gbps HP NIC [29], and one 100 Gbps Mellanox ConnectX5 NIC. Our HP NICs are capable of supporting 4×25 Gbps interfaces using a PSM4 transceiver with four breakout fibers [7], enabling us to build a TOPOOPT system with degree $d = 4$ and $B = 25$ Gbps. We enable DCB [18] and PFC on these interfaces to support a lossless fabric for RDMA. To compare TOPOOPT's training performance with an ideal baseline, we connect the Mellanox NICs on each server to a 100 Gbps MX480 Juniper switch [30]. We build a completely functional TOPOOPT-oneshot prototype with our patch panel, including 1×2 optical switches [98] to flip between active/look-ahead topologies. Figure 17 shows our prototype. Given that our simulation results suggest the reconfiguration latency of OCS is too long for TOPOOPT-reconfig, we only focus on TOPOOPT-oneshot in our prototype.

Distributed training framework. We use FlexFlow's training engine [26], based on Legion's parallel programming system [31], to train three DNN models: ResNet50 [70], BERT [58], and CANDLE [3]. Since our prototype is an order of magnitude smaller scale than our simulation setup, we use smaller model sizes and batch sizes. Table 4 lists the details of each model. We ensure all GPUs are fully utilized.
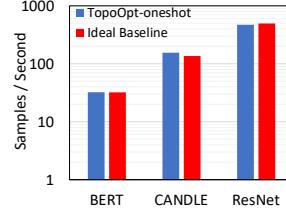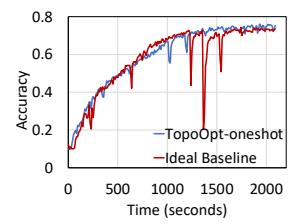
Modifications to NCCL. By default, the NCCL communication library [36] assumes all network interfaces are routable from other interfaces. This assumption is not ideal for TOPOOPT because we have a specific routing strategy to optimize training time. We modify NCCL to understand TOPOOPT's topology and respect its routing preferences. Moreover, we integrate our TotientPermsAllReduce permutations into NCCL and enable it to load-balance parameter synchronization across multiple ring-AllReduce permutations.

RDMA indirect forwarding. To support a multihop TOPOOPT interconnect, we enable RDMA RoCEv2 indirect forwarding on all our HP NICs. This is challenging because packet processing and memory access in RDMA protocol is offloaded to the NIC. Hence, if a packet's IP destination address does not match the NIC's IP address, RDMA engine silently drops the packet. Hence, by default, RDMA does not support host-level indirect forwarding for a host to act as a relay for other hosts. To address this issue, we collaborated with engineers from Marvell, the provider of the ASIC on our HP NICs, to adjust the NIC firmware and enable supporting indirect forwarding functionality. Our approach does not require proprietary software/firmware and is applicable to commodity NICs with the same ASIC. We will release our scripts publicly. At a high-level, we use a feature called *NPAR*, or *network partitioning* allowing us to split each 25 Gbps physical interface into two *logical interfaces* in the hardware level: if_1 and if_2. Each logical interface has a different MAC address but only if_1 has an IP address. RDMA is enabled on if_1 but disabled on if_2. Hence, packets arriving at if_2 are delivered to the host networking stack. We then establish a set of `iproute`, `arp`, and `tc flower` rules in Linux to guarantee that a packet is routed to if_1 logical interface if its destination IP address matches if_1's IP address. Otherwise, the packet is handled by if_2, allowing the NIC to give the packet to the Linux kernel for further processing. Compared to pure point-to-point RDMA, this approach takes a small performance penalty, but our experiments show the overhead is negligible. A more performant produc-

tion implementation can use *XDP* (eXpress Data Path) [25] to increase efficiency. Moreover, the future generation of Marvell ASICs will support hardware offloading of *tc flower* [28]; this will further reduce the performance penalty of our approach, since the NIC can handle indirect forwarding packets.

Training performance. Figure 18 demonstrates that TOPOOPT achieves a training throughput (samples/second) similar to that of our ideal baseline. Moreover, Figure 19 shows that our prototype and baseline have a similar time-to-accuracy for training ResNet50 on the CIFAR10 dataset [80]. The small differences between the time-to-accuracy curves are due to random seed selection.

7 Discussion

Handling scale. A flat TOPOOPT cluster with OCSs can scale to 384 servers and a TOPOOPT cluster with patch panels can scale to 1000 servers. Assuming each server has 8 GPUs, these clusters can host 3,072 and 8,000 GPUs, respectively. Given that our DNN jobs run on less than 1000 workers (Figure 1a), there is no immediate need to create a hierarchy of switches. To further scale a TOPOOPT cluster, we can create a hierarchical interconnect by placing the servers under ToR switches and connecting the ToR switches to the optical switch layer, similar to prior work [50, 67, 68, 88]. Another option is to build a Clos topology using a hierarchy of optical switches and patch panels. We leave exploring these options to future work.

Supporting dynamic scheduling and elasticity. Prior work has demonstrated the benefits of dynamically choosing the training servers for elastic training jobs [86, 100]. Our target usecase in BIGNET is to leverage TOPOOPT for the vast number of long-lasting training jobs that do not change dynamically. In cases where elasticity is required, instead of using patch panels, we use OCSs (or other fast reconfigurable optical switches) to change the servers participating in a job quickly. Note that dynamically changing the set of servers participating in a job while keeping both the topology and the parallelization strategy optimal requires augmenting the optimization space with an additional dimension, hence, making the problem even more challenging, which we leave to future work.

Handling failures. Unlike SiP-ML's single ring topology [79], our TOPOLOGYFINDER's technique spreads the available degree across servers to create topologies with a diverse set of AllReduce permutations, which, in turn, increases the failure resiliency of a TOPOOPT interconnect. In particular, a TOPOOPT topology does not have a single point of failure.

Supporting multi-tenancy. To support multi-tenancy [122, 123], TOPOOPT can leverage NVIDIA's MIG [38] to treat one physical server as multiple logical servers in its topology.

TotientPerms in Fat-trees. Although our TotientPerms technique is well-suited for reconfigurable optical interconnects, it may be of independent interest for Fat-tree interconnects as well since load-balancing the AllReduce traffic across multiple permutations can help with network congestion.

8 Related Work

Optimizing DNN training. To address the increasing computation and network bandwidth requirements of large training jobs, a plethora of frameworks have been proposed [4, 44, 55, 65, 71, 73, 76, 77, 93, 96, 97, 105, 109, 116, 125]. These frameworks distribute the dataset and/or DNN model across accelerators while considering the available network bandwidth, but unlike TOPOOPT, they do not consider the *physical layer topology* as an optimization dimension. Specifically, Blink [116] builds fast collectives for distributed ML, but it needs a physical topology to generate its spanning trees. Moreover, several methods have been proposed to quantize and compress the gradients to reduce the amount of communication data across servers [46, 52, 124]. While all these approaches are effective, they are designed for data parallel strategies and do not consider the large amount of data transfers caused by model parallel training. Wang et al. [118] compared the performance of Fat-trees and BCube topologies for distributed training workloads and highlighted several inefficiencies in Fat-trees. However, unlike TOPOOPT, their proposed approach does not co-optimize topology and parallelization strategy.

DNN parallelization strategies. Data and model parallelism have been widely used by today's DNN frameworks (e.g., TensorFlow [42], PyTorch [40], MXNet [15]) to parallelize training across multiple devices. Recent work has also proposed *automated frameworks* (e.g., FlexFlow [76], ColocRL [89]) that find efficient parallelization strategies by searching over a comprehensive space of potential strategies. These frameworks rely on and are optimized for the conventional Fat-tree interconnects. TOPOOPT proposes a new approach to building DNN training systems by jointly optimizing network topology and parallelization strategy.

DNN training infrastructures and schedulers. Several training infrastructures have been proposed recently, including NVIDIA DGX SuperPOD [9], TPU cluster [8], and supercomputers [1]. All these systems assume non-reconfigurable network topologies, such as Fat-tree, Torus, and other traffic oblivious interconnects. TOPOOPT is the first DNN system that uses commodity reconfigurable interconnects to accelerate DNN jobs. Gandiva [120], Themis [86], Tiresias [66], BytePS [77, 97], and Pollux [100] seek to improve the utilization of GPU clusters through scheduling algorithms. These approaches are complementary to ours, and many of their techniques can be applied to a TOPOOPT cluster.

Optical Interconnects. Several papers demonstrated the benefits of optically reconfigurable interconnects for datacenters [50, 53, 57, 60, 64, 83–85, 87, 88, 99]. As mentioned in Section 3.3, these designs lead to sub-optimal topologies for distributed DNN traffic. Similarly, *traffic oblivious* interconnects, such as RotorNet [87, 88], are a great fit for datacenter workloads, but they are not suitable for DNN training jobs characterized by repetitive AllReduce and MP traffic demands. Hybrid electrical/optical datacenter proposals [60, 117] can be

used to route AllReduce traffic through the optical fabric and MP flows through a standard electrical Fat-tree network. But hybrid clusters are not cost effective and suffer from many problems, including TCP ramp-up inefficiencies [91], segregated routing issues [61], and uncertainty in terms of how to divide the cluster between electrical and optical fabrics [64, 68].

9   Conclusion

We present TOPOOPT, a novel network interconnect to build DNN training clusters. We design an alternating optimization algorithm that explores the large space of *Computation* × *Communication* × *Topology* strategies for a DNN workload, and demonstrate TOPOOPT obtains up to 3× faster training iteration time than a cost-equivalent Fat-tree.

References

[1] Summit Supercomputer, 2014. https://www.olcf.ornl.gov/summit/.

[2] Baidu, 2017. https://github.com/baidu-research/baidu-allreduce.

[3] CANDLE Uno: Predicting Tumor Dose Response across Multiple Data Sources, 2017. https://github.com/ECP-CANDLE/Benchmarks/tree/master/Pilot1/Uno.

[4] Meet Horovod: Uber's Open Source Distributed Deep Learning Framework for TensorFlow, 2017. https://eng.uber.com/horovod.

[5] htsim packet simulator, 2018. https://github.com/nets-cs-pub-ro/NDP/wiki/NDP-Simulator.

[6] CANcer Distributed Learning Environment (CANDLE), 2019. https://datascience.cancer.gov/collaborations/joint-design-advanced-computing/candle.

[7] AOI 100G PSM4 Transceiver, 2020. https://www.ebay.com/itm/234092018446?hash=item3680f8bb0e:g:WoMAAOSwLFJg8dKF.

[8] Google TPU, 2020. https://cloud.google.com/tpu.

[9] Nvidia DGX SuperPOD, 2020. https://www.nvidia.com/en-us/data-center/dgx-superpod/.

[10] NVIDIA is Preparing Co-Packaged Photonics for NVLink, Dec. 2020. https://www.techpowerup.com/276139/nvidia-is-preparing-co-packaged-photonics-for-nvlink.

[11] 100GBASE-SR4 QSFP28 850nm 100m DOM MTP/MPO MMF Optical Transceiver Module, 2021. https://www.fs.com/products/48354.html.

[12] 10GBASE-SR SFP+ 850nm 300m DOM LC MMF Transceiver Module, 2021. https://www.fs.com/products/11552.html.

[13] 25GBASE-SR SFP28 850nm 100m DOM LC MMF Optical Transceiver Module, 2021. https://www.fs.com/products/67991.html.

[14] 40GBASE-SR4 QSFP+ 850nm 150m DOM MTP/MPO MMF Optical Transceiver Module, 2021. https://www.fs.com/products/36143.html.

[15] Apache MXNet, 2021. https://mxnet.apache.org/.

[16] Calient Optical Circuit Switch, 2021. https://www.calient.net/products/edge640-optical-circuit-switch/.

[17] Chelsio T540-LP-CR 4-Port 10 Gigabit Ethernet Adapter Card - Part ID: T540-LP-CR, 2021. https://www.colfaxdirect.com/store/pc/viewPrd.asp?idproduct=3526&idcategory=6.

[18] Data Center Bridging eXchange (DCBX), 2021. https://man7.org/linux/man-pages/man8/dcb-dcbx.8.html.

[19] Datasheet for Single Mode Network Optical Switch up to 384x384 ports, 2021. https://www.hubersuhner.com/en/documents-repository/technologies/pdf/data-sheets-optical-switches/polatis-series-7000n.

[20] Deep Learning Recommendation Model for Personalization and Recommendation Systems, 2021. https://github.com/facebookresearch/dlrm.

[21] Edgecore AS5610-52X 48-Port 10GbE Bare Metal Switch with ONIE - Part ID: 5610-52X-O-AC-F-US, 2021. https://www.colfaxdirect.com/store/pc/viewPrd.asp?idproduct=3025&idcategory=7.

[22] Edgecore AS6712-32X 32-Port 40GbE Bare Metal Switch with ONIE - Part ID: 6712-32X-O-12V-F, 2021. https://www.colfaxdirect.com/store/pc/viewPrd.asp?idproduct=3602&idcategory=7.

[23] Edgecore AS7312-54XS 48-Port 25GbE + 6-Port 100GbE Bare Metal Switch with ONIE - Part ID: 7312-54XS-O-AC-F-US, 2021. https://www.colfaxdirect.com/store/pc/viewPrd.asp?idproduct=3598&idcategory=7.

[24] Edgecore AS7816-64X 64-Port 100GbE Bare Metal Switch with ONIE - Part ID: 7816-64X-O-AC-B-US, 2021. https://www.colfaxdirect.com/store/pc/viewPrd.asp?idproduct=3483&idcategory=7.

[25] eXpress Data Path, 2021. https://xdp-project.net/.

[26] Flex Flow's Training Engine, 2021. https://flexflow.ai/.

[27] FlexFlow source code, 2021. https://github.com/flexflow/FlexFlow.

[28] Flow based traffic control filter, 2021. https://man7.org/linux/man-pages/man8/tc-flower.8.html.

[29] HPE Ethernet 4x25Gb 1-port 620QSFP28 Adapter, 2021. https://support.hpe.com/hpesc/public/docDisplay?docId=emr_na-c05220334.

[30] Juniper MX480 switch, 2021. https://www.juniper.net/us/en/products/routers/mx-series/mx480-universal-routing-platform/specs.html.

[31] Legion Programming System, 2021. https://legion.stanford.edu/overview/.

[32] Mellanox ConnectX-4 Single Port 10 Gigabit Ethernet Adapter Card, PCIe 3.0 x8 - Part ID: MCX4111A-XCAT, 2021. https://www.colfaxdirect.com/store/pc/viewPrd.asp?idproduct=2812&idcategory=6.

[33] Mellanox ConnectX-4 Single Port 25 Gigabit Ethernet Adapter Card, PCIe 3.0 x8 - Part ID: MCX4111A-ACAT, 2021. https://www.colfaxdirect.com/store/pc/viewPrd.asp?idproduct=2814&idcategory=6.

[34] Mellanox ConnectX-5 EN Single Port 100 Gigabit Ethernet Adapter Card, PCIe 3.0 x16 - Part ID: MCX515A-CCAT, 2021. https://www.colfaxdirect.com/store/pc/viewPrd.asp?idproduct=3150&idcategory=6.

[35] Mellanox ConnectX-6 VPI Single Port HDR 200Gb/s InfiniBand & Ethernet Adapter Card, PCIe 3.0/4.0 x16 - Part ID: MCX653105A-HDAT, 2021. https://www.colfaxdirect.com/store/pc/viewPrd.asp?idproduct=3669&idcategory=6.

[36] NCCL, 2021. https://github.com/NVIDIA/nccl-tests.

[37] NVIDIA A100 Tensor Core GPU, 2021. https://www.nvidia.com/en-us/data-center/a100/.

[38] NVIDIA MULTI-INSTANCE GPU, 2021. https://www.nvidia.com/en-us/technologies/multi-instance-gpu/.

[39] Polatis Optical Circuit Switch, 2021. https://www.polatis.com/series-7000-384x384-port-software-controlled-optical-circuit-switch-sdn-enabled.asp.

[40] PyTorch, 2021. https://pytorch.org.

[41] Telescent G4 Network Topology Manager, 2021. https://www.telescent.com/products.

[42] Martín Abadi, Paul Barham, Jianmin Chen, Zhifeng Chen, Andy Davis, Jeffrey Dean, Matthieu Devin, Sanjay Ghemawat, Geoffrey Irving, Michael Isard, Manjunath Kudlur, Josh Levenberg, Rajat Monga, Sherry Moore, Derek G. Murray, Benoit Steiner, Paul Tucker, Vijay Vasudevan, Pete Warden, Martin Wicke, Yuan Yu, and Xiaoqiang Zheng. Tensorflow: A system for large-scale machine learning. In *12th USENIX Symposium on Operating Systems Design and Implementation (OSDI 16)*, pages 265–283, Savannah, GA, November 2016. USENIX Association.

[43] Bilge Acun, Matthew Murphy, Xiaodong Wang, Jade Nie, Carole-Jean Wu, and Kim Hazelwood. Understanding training efficiency of deep learning recommendation models at scale, 2020.

[44] Ravichandra Addanki, Shaileshh Bojja Venkatakrishnan, Shreyan Gupta, Hongzi Mao, and Mohammad Alizadeh. Learning generalizable device placement algorithms for distributed machine learning. In *Advances in Neural Information Processing Systems*, volume 32, pages 3981–3991. Curran Associates, Inc., 2019.

[45] Mohammad Al-Fares, Alexander Loukissas, and Amin Vahdat. A scalable, commodity data center network architecture. *SIGCOMM Comput. Commun. Rev.*, 38(4):63–74, August 2008.

[46] Dan Alistarh, Demjan Grubic, Jerry Li, Ryota Tomioka, and Milan Vojnovic. Qsgd: Communication-efficient sgd via gradient quantization and encoding. In I. Guyon, U. V. Luxburg, S. Bengio, H. Wallach, R. Fergus, S. Vishwanathan, and R. Garnett, editors, *Advances in Neural Information Processing Systems*, volume 30, pages 1709–1720. Curran Associates, Inc., 2017.

[47] Mohammad Alizadeh, Albert Greenberg, David A. Maltz, Jitendra Padhye, Parveen Patel, Balaji Prabhakar, Sudipta Sengupta, and Murari Sridharan. Data Center TCP (DCTCP). In *Proceedings of the ACM SIGCOMM 2010 Conference*, SIGCOMM '10, pages 63–74, New York, NY, USA, 2010. ACM.

[48] Mohammad Alizadeh, Shuang Yang, Milad Sharif, Sachin Katti, Nick McKeown, Balaji Prabhakar, and Scott Shenker. pfabric: Minimal near-optimal datacenter transport. In *Proceedings of the ACM SIGCOMM 2013 Conference on SIGCOMM*, SIGCOMM '13, pages 435–446, New York, NY, USA, 2013. ACM.

[49] Javed A. Aslam. Dynamic Programming Solution to the Coin Changing Problem, 2004. https://www.ccs.neu.edu/home/jaa/CSG713.04F/Information/Handouts/dyn_prog.pdf.

[50] Hitesh Ballani, Paolo Costa, Raphael Behrendt, Daniel Cletheroe, Istvan Haller, Krzysztof Jozwik, Fotini Karinou, Sophie Lange, Kai Shi, Benn Thomsen, and Hugh Williams. Sirius: A flat datacenter network with nanosecond optical switching. In *Proceedings of the Annual Conference of the ACM Special Interest Group on Data Communication on the Applications, Technologies, Architectures, and Protocols for Computer Communication*, SIGCOMM '20, page 782–797, New York, NY, USA, 2020. Association for Computing Machinery.

[51] Theophilus Benson, Aditya Akella, and David A. Maltz. Network traffic characteristics of data centers in the wild. In *Proceedings of the 10th ACM SIGCOMM Conference on Internet Measurement*, IMC '10, pages 267–280, New York, NY, USA, 2010. ACM.

[52] Chia-Yu Chen, Jungwook Choi, Daniel Brand, Ankur Agrawal, Wei Zhang, and Kailash Gopalakrishnan. Adacomp : Adaptive residual gradient compression for data-parallel distributed training. *Thirty-Second AAAI Conference on Artificial Intelligence*, 2018.

[53] Li Chen, Kai Chen, Zhonghua Zhu, Minlan Yu, George Porter, Chunming Qiao, and Shan Zhong. Enabling wide-spread communications on optical fabric with megaswitch. In *14th USENIX Symposium on Networked Systems Design and Implementation (NSDI 17)*, pages 577–593, Boston, MA, 2017. USENIX Association.

[54] Qixiang Cheng, Richard Dai, Meisam Bahadori, Nathan C. Abrams, Padraic E Morrissey, Madeleine Glick, Peter O'Brien, and Keren Bergman. Si/sin microring-based optical router in switch-and-select topology. 09 2018.

[55] Minsik Cho, Ulrich Finkler, David Kung, and Hillery Hunter. Blueconnect: Decomposing all-reduce for deep learning on heterogeneous network hierarchy. SysML Conference, 2019.

[56] Eric Chung, Jeremy Fowers, Kalin Ovtcharov, Michael Papamichael, Adrian Caulfield, Todd Massengil, Ming Liu, Daniel Lo, Shlomi Alkalay, and Michael Haselman. Accelerating persistent neural networks at datacenter scale. In *Hot Chips*, volume 29, 2017.

[57] K. Clark, H. Ballani, P. Bayvel, D. Cletheroe, T. Gerard, I. Haller, K. Jozwik, K. Shi, B. Thomsen, P. Watts, H. Williams, G. Zervas, P. Costa, and Z. Liu. Sub-nanosecond clock and data recovery in an optically-switched data centre network. In *2018 European Conference on Optical Communication (ECOC)*, pages 1–3, 2018.

[58] Jacob Devlin, Ming-Wei Chang, Kenton Lee, and Kristina Toutanova. BERT: pre-training of deep bidirectional transformers for language understanding. *CoRR*, abs/1810.04805, 2018.

[59] Jack Edmonds. Paths, trees, and flowers. *Canadian Journal of Mathematics*, 17:449–467, 1965.

[60] Nathan Farrington, George Porter, Sivasankar Radhakrishnan, Hamid Hajabdolali Bazzaz, Vikram Subramanya, Yeshaiahu Fainman, George Papen, and Amin Vahdat. Helios: A hybrid electrical/optical switch architecture for modular data centers. *SIGCOMM'10*, pages 339–350.

[61] K. Foerster, M. Ghobadi, and S. Schmid. Characterizing the algorithmic complexity of reconfigurable data center architectures. In *Proc. ANCS '18*, pages 89–96, 2018.

[62] Everest G. and Ward Thomas. An introduction to number theory, 2005.

[63] Peter X. Gao, Akshay Narayan, Sagar Karandikar, Joao Carreira, Sangjin Han, Rachit Agarwal, Sylvia Ratnasamy, and Scott Shenker. Network requirements for resource disaggregation. In *Proceedings of the 12th USENIX Conference on Operating Systems Design and Implementation*, OSDI'16, pages 249–264, Berkeley, CA, USA, 2016. USENIX Association.

[64] Monia Ghobadi, Ratul Mahajan, Amar Phanishayee, Nikhil Devanur, Janardhan Kulkarni, Gireeja Ranade, Pierre-Alexandre Blanche, Houman Rastegarfar, Madeleine Glick, and Daniel Kilper. Projector: Agile reconfigurable data center interconnect. In *Proceedings of the 2016 ACM SIGCOMM Conference*, SIGCOMM '16, pages 216–229, New York, NY, USA, 2016. Association for Computing Machinery.

[65] Priya Goyal, Piotr Dollár, Ross B. Girshick, Pieter Noordhuis, Lukasz Wesolowski, Aapo Kyrola, Andrew Tulloch, Yangqing Jia, and Kaiming He. Accurate, large minibatch SGD: training imagenet in 1 hour. *CoRR*, abs/1706.02677, 2017.

[66] Juncheng Gu, Mosharaf Chowdhury, Kang G. Shin, Yibo Zhu, Myeongjae Jeon, Junjie Qian, Hongqiang Liu, and Chuanxiong Guo. Tiresias: A GPU cluster manager for distributed deep learning. In *16th USENIX Symposium on Networked Systems Design and Implementation (NSDI 19)*, pages 485–500, Boston, MA, February 2019. USENIX Association.

[67] Chuanxiong Guo, Guohan Lu, Dan Li, Haitao Wu, Xuan Zhang, Yunfeng Shi, Chen Tian, Yongguang Zhang, and Songwu Lu. Bcube: A high performance, server-centric network architecture for modular data centers. In *Proceedings of the ACM SIGCOMM 2009 Conference on Data Communication*, SIGCOMM '09, page 63–74, New York, NY, USA, 2009. Association for Computing Machinery.

[68] Navid Hamedazimi, Zafar Qazi, Himanshu Gupta, Vyas Sekar, Samir R. Das, Jon P. Longtin, Himanshu Shah, and Ashish Tanwer. Firefly: A reconfigurable wireless data center fabric using free-space optics. *SIGCOMM'14*, pages 319–330.

[69] Sayed Hadi Hashemi, Sangeetha Abdu Jyothi, and Roy H. Campbell. Communication scheduling as a first-class citizen in distributed machine learning systems. *CoRR*, abs/1803.03288, 2018.

[70] Kaiming He, Xiangyu Zhang, Shaoqing Ren, and Jian Sun. Deep residual learning for image recognition. In *Proceedings of the IEEE conference on computer vision and pattern recognition*, pages 770–778, 2016.

[71] Yanping Huang, Yonglong Cheng, Dehao Chen, HyoukJoong Lee, Jiquan Ngiam, Quoc V. Le, and Zhifeng Chen. Gpipe: Efficient training of giant neural networks using pipeline parallelism. *NeurIPS*, 2019.

[72] Yanping Huang, Youlong Cheng, Ankur Bapna, Orhan Firat, Mia Xu Chen, Dehao Chen, HyoukJoong Lee, Jiquan Ngiam, Quoc V. Le, Yonghui Wu, and Zhifeng Chen. Gpipe: Efficient training of giant neural networks using pipeline parallelism, 2019.

[73] Forrest N. Iandola, Khalid Ashraf, Matthew W. Moskewicz, and Kurt Keutzer. Firecaffe: near-linear acceleration of deep neural network training on compute clusters. *CoRR*, abs/1511.00175, 2015.

[74] Anand Jayarajan, Jinliang Wei, Garth Gibson, Alexandra Fedorova, and Gennady Pekhimenko. Priority-based parameter propagation for distributed DNN training. *CoRR*, abs/1905.03960, 2019.

[75] Xianyan Jia, Shutao Song, Wei He, Yangzihao Wang, Haidong Rong, Feihu Zhou, Liqiang Xie, Zhenyu Guo, Yuanzhou Yang, Liwei Yu, Tiegang Chen, Guangxiao Hu, Shaohuai Shi, and Xiaowen Chu. Highly scalable deep learning training system with mixed-precision: Training imagenet in four minutes. *CoRR*, abs/1807.11205, 2018.

[76] Zhihao Jia, Matei Zaharia, and Alex Aiken. Beyond data and model parallelism for deep neural networks. *SysML*, 2019.

[77] Yimin Jiang, Yibo Zhu, Chang Lan, Bairen Yi, Yong Cui, and Chuanxiong Guo. A unified architecture for accelerating distributed DNN training in heterogeneous gpu/cpu clusters. In *14th USENIX Symposium on Operating Systems Design and Implementation (OSDI 20)*, pages 463–479. USENIX Association, November 2020.

[78] A. S. Kewitsch. Large scale, all-fiber optical cross-connect switches for automated patch-panels. *Journal of Lightwave Technology*, 27(15):3107–3115, 2009.

[79] Mehrdad Khani, Manya Ghobadi, Mohammad Alizadeh, Ziyi Zhu, Madeleine Glick, Keren Bergman, Amin Vahdat, Benjamin Klenk, and Eiman Ebrahimi. Sip-ml: High-bandwidth optical network interconnects for machine learning training. In *Proceedings of the 2021 ACM SIGCOMM 2021 Conference*, SIGCOMM '21, pages 657–675, New York, NY, USA, 2021. Association for Computing Machinery.

[80] Alex Krizhevsky, Geoffrey Hinton, et al. Learning multiple layers of features from tiny images. 2009.

[81] Mu Li, David G. Andersen, Jun Woo Park, Alexander J. Smola, Amr Ahmed, Vanja Josifovski, James Long, Eugene J. Shekita, and Bor-Yiing Su. Scaling distributed machine learning with the parameter server. OSDI'14, pages 583–598. USENIX Association, 2014.

[82] Yujun Lin, Song Han, Huizi Mao, Yu Wang, and William J Dally. Deep gradient compression: Reducing the communication bandwidth for distributed training. *arXiv preprint arXiv:1712.01887*, 2017.

[83] He Liu, Feng Lu, Alex Forencich, Rishi Kapoor, Malveeka Tewari, Geoffrey M. Voelker, George Papen, Alex C. Snoeren, and George Porter. Circuit switching under the radar with REACToR. *NSDI'14*, pages 1–15.

[84] He Liu, Matthew K. Mukerjee, Conglong Li, Nicolas Feltman, George Papen, Stefan Savage, Srinivasan Seshan, Geoffrey M. Voelker, David G. Andersen, Michael Kaminsky, George Porter, and Alex C. Snoeren. Scheduling techniques for hybrid circuit/packet networks. In *Proceedings of the 11th ACM Conference on Emerging Networking Experiments and Technologies*, CoNEXT '15, New York, NY, USA, 2015. Association for Computing Machinery.

[85] Yunpeng James Liu, Peter Xiang Gao, Bernard Wong, and Srinivasan Keshav. Quartz: A new design element for low-latency dcns. *SIGCOMM'14*, pages 283–294.

[86] Kshiteej Mahajan, Arjun Balasubramanian, Arjun Singhvi, Shivaram Venkataraman, Aditya Akella, Amar Phanishayee, and Shuchi Chawla. Themis: Fair and efficient GPU cluster scheduling. In *17th USENIX Symposium on Networked Systems Design and Implementation (NSDI 20)*, pages 289–304, Santa Clara, CA, February 2020. USENIX Association.

[87] William M. Mellette, Rajdeep Das, Yibo Guo, Rob McGuinness, Alex C. Snoeren, and George Porter. Expanding across time to deliver bandwidth efficiency and low latency. *NSDI'20*, 2020.

[88] William M. Mellette, Rob McGuinness, Arjun Roy, Alex Forencich, George Papen, Alex C. Snoeren, and George Porter. Rotornet: A scalable, low-complexity, optical datacenter network. *SIGCOMM '17*, pages 267–280, 2017.

[89] Azalia Mirhoseini, Hieu Pham, Quoc V. Le, Benoit Steiner, Rasmus Larsen, Yuefeng Zhou, Naveen Kumar, Mohammad Norouzi, Samy Bengio, and Jeff Dean. Device placement optimization with reinforcement learning. In Doina Precup and Yee Whye Teh, editors, *Proceedings of the 34th International Conference on Machine Learning*, volume 70 of *Proceedings of Machine Learning Research*, pages 2430–2439, International Convention Centre, Sydney, Australia, 06–11 Aug 2017. PMLR.

[90] Dheevatsa Mudigere, Yuchen Hao, Jianyu Huang, Zhihao Jia, Andrew Tulloch, Srinivas Sridharan, Xing Liu, Mustafa Ozdal, Jade Nie, Jongsoo Park, Liang Luo, Jie Amy Yang, Leon Gao, Dmytro Ivchenko, Aarti Basant, Yuxi Hu, Jiyan Yang, Ehsan K. Ardestani, Xiaodong Wang, Rakesh Komuravelli, Ching-Hsiang Chu, Serhat Yilmaz, Huayu Li, Jiyuan Qian, Zhuobo Feng, Yinbin Ma, Junjie Yang, Ellie Wen, Hong Li, Lin Yang, Chonglin Sun, Whitney Zhao, Dimitry Melts, Krishna Dhulipala, KR Kishore, Tyler Graf, Assaf Eisenman, Kiran Kumar Matam, Adi Gangidi, Guoqiang Jerry Chen, Manoj Krishnan, Avinash Nayak, Krishnakumar Nair, Bharath Muthiah, Mahmoud khorashadi, Pallab Bhattacharya, Petr Lapukhov, Maxim Naumov, Lin Qiao, Mikhail Smelyanskiy, Bill Jia, and Vijay Rao. Software-hardware co-design for fast and scalable training of deep learning recommendation models, 2021.

[91] Matthew K. Mukerjee, Christopher Canel, Weiyang Wang, Daehyeok Kim, Srinivasan Seshan, and Alex C. Snoeren. Adapting TCP for reconfigurable datacenter networks. In *17th USENIX Symposium on Networked Systems Design and Implementation (NSDI 20)*, pages 651–666, Santa Clara, CA, February 2020. USENIX Association.

[92] Shar Narasimhan. NVIDIA Clocks World's Fastest BERT Training Time and Largest Transformer Based Model, Paving Path For Advanced Conversational AI, Aug. 2019. https://devblogs.nvidia.com/training-bert-with-gpus/.

[93] Deepak Narayanan, Aaron Harlap, Amar Phanishayee, Vivek Seshadri, Nikhil R. Devanur, Gregory R. Ganger, Phillip B. Gibbons, and Matei Zaharia. Pipedream: Generalized pipeline parallelism for dnn training. In *Proceedings of the 27th ACM Symposium on Operating Systems Principles*, SOSP'19, pages 1–15, New York, NY, USA, 2019. Association for Computing Machinery.

[94] Maxim Naumov, John Kim, Dheevatsa Mudigere, Srinivas Sridharan, Xiaodong Wang, Whitney Zhao, Serhat Yilmaz, Changkyu Kim, Hector Yuen, Mustafa Ozdal, Krishnakumar Nair, Isabel Gao, Bor-Yiing Su, Jiyan Yang, and Mikhail Smelyanskiy. Deep learning training in facebook data centers: Design of scale-up and scale-out systems, 2020.

[95] Maxim Naumov, Dheevatsa Mudigere, Hao-Jun Michael Shi, Jianyu Huang, Narayanan Sundaraman, Jongsoo Park, Xiaodong Wang, Udit Gupta, Carole-Jean Wu, Alisson G. Azzolini, Dmytro Dzhulgakov, Andrey Mallevich, Ilia Cherniavskii, Yinghai Lu, Raghuraman Krishnamoorthi, Ansha Yu, Volodymyr Kondratenko, Stephanie Pereira, Xianjie Chen, Wenlin Chen, Vijay Rao, Bill Jia, Liang Xiong, and Misha Smelyanskiy. Deep learning recommendation model for personalization and recommendation systems, 2019.

[96] T. T. Nguyen, M. Wahib, and R. Takano. Topology-aware sparse allreduce for large-scale deep learning. In *2019 IEEE 38th International Performance Computing and Communications Conference (IPCCC)*, pages 1–8, 2019.

[97] Yanghua Peng, Yibo Zhu, Yangrui Chen, Yixin Bao, Bairen Yi, Chang Lan, Chuan Wu, and Chuanxiong Guo. A generic communication scheduler for distributed dnn training acceleration. In *Proceedings of the 27th ACM Symposium on Operating Systems Principles*, SOSP '19, page 16–29, New York, NY, USA, 2019. Association for Computing Machinery.

[98] Genzhi Photonics. 1x2 Mechanical Optical Switch, 2021. https://www.gezhiphotonics.com/1x2-optical-switch.html.

[99] George Porter, Richard Strong, Nathan Farrington, Alex Forencich, Pang Chen-Sun, Tajana Rosing, Yeshaiahu Fainman, George Papen, and Amin Vahdat. Integrating microsecond circuit switching into the data center. *SIGCOMM'13*, pages 447–458.

[100] Aurick Qiao, Sang Keun Choe, Suhas Jayaram Subramanya, Willie Neiswanger, Qirong Ho, Hao Zhang, Gregory R. Ganger, and Eric P. Xing. Pollux: Co-adaptive cluster scheduling for goodput-optimized deep learning. In *15th USENIX Symposium on Operating Systems Design and Implementation (OSDI 21)*, pages 1–18. USENIX Association, July 2021.

[101] J. R. Quinlan. Induction of decision trees. *Mach. Learn.*, 1(1):81–106, March 1986.

[102] Leslie Reid. MOX Announces New Telescent Automation Technology on Its Latest Hillsboro to Portland Fiber Route, Sept. 2020. https://www.businesswire.com/news/home/20200915005391/en/MOX-Announces-New-Telescent-Automation-Technology-on-Its-Latest-Hillsboro-to-Portland-Fiber-Route.

[103] Peter Sanders, Jochen Speck, and Jesper Larsson Träff. Two-tree algorithms for full bandwidth broadcast, reduction and scan. *Parallel Computing*, 35(12):581–594, 2009.

[104] Tae Joon Seok, Niels Quack, Sangyoon Han, Richard S. Muller, and Ming C. Wu. Large-scale broadband digital silicon photonic switches with vertical adiabatic couplers. *Optica*, 3(1):64–70, Jan 2016.

[105] Alexander Sergeev and Mike Del Balso. Horovod: fast and easy distributed deep learning in tensorflow. *CoRR*, abs/1802.05799, 2018.

[106] Mohammad Shoeybi, Mostofa Patwary, Raul Puri, Patrick LeGresley, Jared Casper, and Bryan Catanzaro. Megatron-lm: Training multi-billion parameter language models using model parallelism, 2020.

[107] Karen Simonyan and Andrew Zisserman. Very deep convolutional networks for large-scale image recognition, 2015.

[108] Ankit Singla, Chi-Yao Hong, Lucian Popa, and P. Brighten Godfrey. Jellyfish: Networking data centers randomly. In *Proceedings of the 9th USENIX Conference on Networked Systems Design and Implementation*, NSDI'12, pages 17–17, Berkeley, CA, USA, 2012. USENIX Association.

[109] Jakub Tarnawski, Amar Phanishayee, Nikhil R. Devanur, Divya Mahajan, and Fanny Nina Paravecino. Efficient algorithms for device placement of DNN graph operators. In Hugo Larochelle, Marc'Aurelio Ranzato, Raia Hadsell, Maria-Florina Balcan, and Hsuan-Tien Lin, editors, *Advances in Neural Information Processing Systems 33: Annual Conference on Neural Information Processing Systems 2020, NeurIPS 2020, December 6-12, 2020, virtual*, 2020.

[110] Rajeev Thakur, Rolf Rabenseifner, and William Gropp. Optimization of collective communication operations in mpich. *Int. J. High Perform. Comput. Appl.*, 19(1):49–66, February 2005.

[111] Rajeev Thakur, Rolf Rabenseifner, and William Gropp. Optimization of collective communication operations in mpich. *Int. J. High Perform. Comput. Appl.*, 19(1):49–66, February 2005.

[112] Rajeev Thakur, Rolf Rabenseifner, and William Gropp. Optimization of collective communication operations in mpich. *The International Journal of High Performance Computing Applications*, 19(1):49–66, 2005.

[113] Yuichiro Ueno and Rio Yokota. Exhaustive study of hierarchical allreduce patterns for large messages between gpus. In *2019 19th IEEE/ACM International Symposium on Cluster, Cloud and Grid Computing (CCGRID)*, pages 430–439, 2019.

[114] Jakob Uszkorei. Transformer: A Novel Neural Network Architecture for Language Understanding, Aug. 2017. https://ai.googleblog.com/2017/08/transformer-novel-neural-network.html.

[115] Asaf Valadarsky, Gal Shahaf, Michael Dinitz, and Michael Schapira. Xpander: Towards optimal-performance datacenters. In *Proceedings of the 12th International on Conference on Emerging Networking EXperiments and Technologies*, CoNEXT '16, pages 205–219, New York, NY, USA, 2016. ACM.

[116] Guanhua Wang, Shivaram Venkataraman, Amar Phanishayee, Jorgen Thelin, Nikhil Devanur, and Ion Stoica. Blink: Fast and generic collectives for distributed ml. In *Conference on Machine Learning and Systems (MLSys 2020)*, March 2020.

[117] Guohui Wang, David G. Andersen, Michael Kaminsky, Konstantina Papagiannaki, T.S. Eugene Ng, Michael Kozuch, and Michael Ryan. c-Through: Part-time optics in data centers. *SIGCOMM'10*, pages 327–338.

[118] S. Wang, D. Li, J. Geng, Y. Gu, and Y. Cheng. Impact of Network Topology on the Performance of DML: Theoretical Analysis and Practical Factors. In *IEEE INFOCOM 2019 - IEEE Conference on Computer Communications*, pages 1729–1737, 2019.

[119] Pijika Watcharapichat, Victoria Lopez Morales, Raul Castro Fernandez, and Peter Pietzuch. Ako: Decentralised deep learning with partial gradient exchange. *SoCC '16*, 2016.

[120] Wencong Xiao, Romil Bhardwaj, Ramachandran Ramjee, Muthian Sivathanu, Nipun Kwatra, Zhenhua Han, Pratyush Patel, Xuan Peng, Hanyu Zhao, Quanlu Zhang, Fan Yang, and Lidong Zhou. Gandiva: Introspective cluster scheduling for deep learning. In *13th USENIX Symposium on Operating Systems Design and Implementation (OSDI 18)*, pages 595–610, Carlsbad, CA, October 2018. USENIX Association.

[121] Pengtao Xie, Jin Kyu Kim, Yi Zhou, Qirong Ho, Abhimanu Kumar, Yaoliang Yu, and Eric Xing. Lighter-communication distributed machine learning via sufficient factor broadcasting. In *Proceedings of the Thirty-Second Conference on Uncertainty in Artificial Intelligence*, pages 795–804, Arlington, Virginia, USA, 2016. AUAI Press.

[122] Peifeng Yu and Mosharaf Chowdhury. Fine-grained GPU sharing primitives for deep learning applications. In Inderjit S. Dhillon, Dimitris S. Papailiopoulos, and Vivienne Sze, editors, *Proceedings of Machine Learning and Systems 2020, MLSys 2020, Austin, TX, USA, March 2-4, 2020*. mlsys.org, 2020.

[123] Peifeng Yu, Jiachen Liu, and Mosharaf Chowdhury. Fluid: Resource-aware hyperparameter tuning engine. In A. Smola, A. Dimakis, and I. Stoica, editors, *Proceedings of Machine Learning and Systems*, volume 3, pages 502–516, 2021.

[124] Yue Yu, Jiaxiang Wu, and Longbo Huang. Double quantization for communication-efficient distributed optimization. In *Advances in Neural Information Processing Systems*, volume 32, pages 4438–4449. Curran Associates, Inc., 2019.

[125] H. Zhao and J. Canny. Kylix: A sparse allreduce for commodity clusters. In *2014 43rd International Conference on Parallel Processing*, pages 273–282, 2014.

[126] Danyang Zhuo, Monia Ghobadi, Ratul Mahajan, Amar Phanishayee, Xuan Kelvin Zou, Hang Guan, Arvind Krishnamurthy, and Thomas Anderson. RAIL: A case for redundant arrays of inexpensive links in data center networks. In *14th USENIX Symposium on Networked Systems Design and Implementation (NSDI 17)*, pages 561–576, Boston, MA, March 2017. USENIX Association.

(a) Traffic Heatmap 1   (b) Traffic Heatmap 2   (c) Traffic Heatmap 3
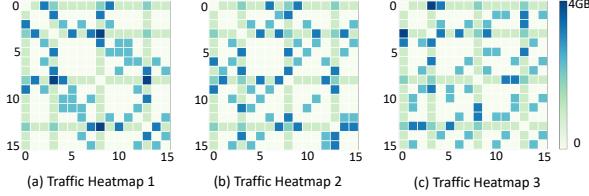
Figure 20: DLRM traffic heatmaps with DBT.

(a) Double binary tree
permutation 1

(b) Double binary tree
permutation 2

(c) Double binary tree
permutation 3
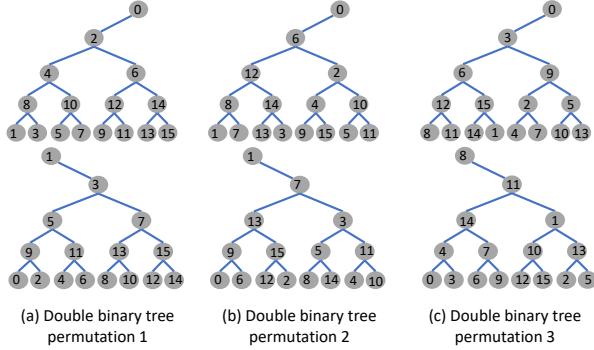
Figure 21: Double binary tree (DBT) permutations.

(a) Traffic Heatmap 1   (b) Traffic Heatmap 2   (c) Traffic Heatmap 3
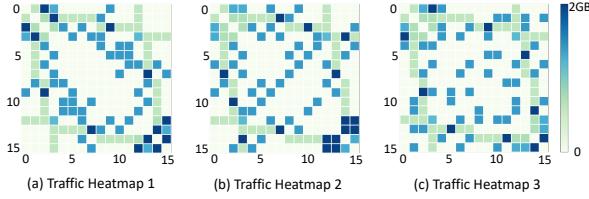
Figure 22: CANDLE traffic heatmaps with DBT.

A   Tree-AllReduce and other AllReduce permutations

Section 2 established that we can manipulate the traffic of a ring-AllReduce collective by permuting the labeling of servers in the AllReduce group. Here, we illustrate how to use the same technique on another AllReduce algorithm, called tree-AllReduce.

In the tree-AllReduce algorithm, the servers are connected logically to form a tree topology. The AllReduce operation happens by first running a reduce operation to the root node with recursive halving, followed by a broadcast to the rest of the cluster with recursive doubling [112].

A common instantiation of tree-AllReduce is the double binary tree (DBT) algorithm described in [103]. In this algorithm, the first step is to create a balanced binary tree for the nodes. The properties of balanced binary trees guarantee that one half of the nodes will be leaf-nodes, and the other half will be in-tree; thus, a second binary tree is constructed by flipping the labeling of the leaf and in-tree nodes. This way, each node (except the root in both trees) has the same amount of communication requirement for the AllReduce operation described in the last paragraph, and bandwidth-optimally is achieved. Figure 21a shows an example where in the first binary tree, the in-tree nodes are even, and the leaf nodes are

odd, while the second tree flips the labeling.

Essentially, the DBT itself is an example of permuting the node labeling to achieve an AllReduce operation with balanced communication load. We also note that we can permute the labeling *for the entire set of nodes* for a pair of DBT to create a new pair of trees that can perform the AllReduce operation at the same speed. Figures 21b and 21c illustrate two other possible double binary trees, and their corresponding traffic demand matrix for the DLRM and CANDLE example shown in Section §2 in Figures 20 and 22. Arbitrary permutations can be used, and to limit the cases, we could simply consider the cyclic permutations in the modular space as described in TotientPerms.

In general, all AllReduce operations can be described as a directed graph $G = (V, E)$ where V is the set of nodes in the cluster, and E denotes data dependencies. The *permutable* property says that every graph $G' = (V, E')$ that is isomorphic to G can perform the AllReduce operation equally well, where the homomorphism between G and G' is described by the symmetric group on V (generally denoted $Sym(V)$ in group theory).

B   Size of AllReduce and MP transfers

In most workloads observed in BIGNET, the size of AllReduce transfers is larger than the size of MP transfers for each iteration. This is because in most cases it would not be worthwhile if MP transfers are as large as AllReduce transfers. Consider the DLRM example in Section 2.2 with 20 GB embedding tables with double-precision floating parameters. If we were to distribute this embedding table using data parallelism, each server would need to send and receive 37.5 GB of data for the AllReduce operation. On a 100 Gbps fabric this would take 3 seconds by itself, where as if we put it on one server, it would only need to transfer 32 MB/server (assume we have a per-server batch size of 8192, then MP traffic is calculated as 16 servers × 8192 samples/server × 512 activation per sample × 8 bytes per activation / 16 servers = 32 MB). We note that adding *pipeline parallelism* can increase the amount of MP traffic as it overlaps forward and backward passes. Efficient ways to pipeline batches remains an active research area [71, 93] especially when hybrid parallelism is employed. Pure model parallelism creates another type of sparse traffic pattern where only accelerators with inter-layer dependencies need to communicate. Our TOPOLOGYFINDER algorithm can support such communication patterns.

On the other hand, conceptually, when the network bandwidth goes to infinity, other overheads in the system (e.g. CUDA kernel launch) will dominate the latency. In such cases, it might be beneficial to choose model parallelism instead of data parallelism, to reduce the amount of system overheads. In particular, prior work showed 10 Tbps Silicon Photonics links enable more aggressive model parallelism where the size of MP traffic is significant [79]. TOPOOPT's approach to distribute the degree between the MP and AllReduce sub-topologies enables us to accommodate this case as well.

Algorithm 3 `CoinChangeMod` pseudocode

1: **procedure** COINCHANGEMOD(N, G)
   ▷ **Input** N: Total number of nodes
   ▷ **Input** G: Network Topology
   ▷ **Output** R: Routings
      ▷ R is the routing result
2:   $R = \{\}$
   ▷ Acquire the set of "coins" from the topology,
   ▷ which are the choices of Algorithm 4
3:   $C = \text{GetCoins}(G)$
4:   **for** $i \in [1, N-1]$ **do**
   ▷ curr_dist denotes the "distance" of a value
   ▷ (node distance) counted by number of "coins"
5:      $curr\_dist[i] = \infty$
   ▷ curr_bt record a back-trace of "coins" to
   ▷ get to a value (node distance)
6:      $curr\_bt[i] = \infty$
7:   **for** $c \in C$ **do**
8:      $curr\_dist[c] = 0$
9:      $curr\_bt[c] = c$
10:   **while** $curr\_dist$ has at least one ∞ in it **do**
11:      **for** $i \in [1, N-1]$ **do**
12:         $new\_dist[i] = curr\_dist[i]$
13:         $new\_bt[i] = curr\_bt[i]$
14:         **for** $c \in C$ **do**
15:            **if** $curr\_dist[(i-c) \bmod N] < new\_dist[i]$ **then**
16:               $new\_dist[i] = cur\_dist[(i-c) \bmod N] + 1$
17:               $new\_bt[i] = c$
18:      $curr\_dist = new\_dist$
19:      $curr\_bt = new\_bt$
   ▷ Construct the routing for each node distance from the back-trace
20:   $R = \text{GetRouteSeq}(curr\_bt)$
21:   **return** R

Algorithm 4 `TopPermutations` pseudocode

1: **procedure** TOPPERMUTATIONS(N, d_k, P_k, T_{MP})
   ▷ **Input** N: Total number of nodes
   ▷ **Input** d_k: Degree allocated for group this AllReduce group of size k
   ▷ **Input** P_k: Candidate permutations for this AllReduce group of size k
   ▷ **Input** T_{mp}: Traffic matrix for MP traffic
   ▷ **Output** G_k: Parameter synchronization topology, as a topology matrix
      ▷ Initially, G_k is empty
2:   $G_k = []$
3:   **for** $k_0 \in P_k$ **do**
      ▷ Pick d_k candidate permutations evenly from starting from k_0
4:      $ProposedConns = \text{Pick\_}d_k(P_k, k_0)$
      ▷ Assert how much MP traffic this choice can satisfy.
      ▷ We want the set of candidates that maximizes the
      ▷ demand satisfied for the MP traffic.
      ▷ The metric of "satisfied MP" can have many definitions
5:      $SatisfiedMP = \text{MPSatisfied}(T_{mp}, ProposedConns)$
6:   $G_k += (\text{The } ProposedConns \text{ that maximizes } SatisfiedMP)$
7:   **return** G_k

Algorithm 2 `TotientPerms` pseudocode

1: **procedure** TOTIENTPERMS(N, k)
   ▷ **Input** N: Total number of nodes
   ▷ **Input** k: AllReduce group size
   ▷ **Output** P_k: Set of permutations for AllReduce group of size k
      ▷ Initially, P_k is empty
2:   $P_k = \{\}$
   ▷ This loop runs $\phi(p)$ times, where
   ▷ ϕ is the Euler Totient function, $\phi(p) = |\{k < p : gcd(k, p) = 1\}|$
   ▷ one can also restrict p to be prime only
3:   **for** $p \leq k, gcd(p, k) == 1$ **do**
4:      $one\_perm = []$
5:      **for** i in 0 to N/k **do**
6:         $one\_perm += [i + j \times p \textbf{ for } j \text{ in 0 to } k]$
7:      $P_k += one\_perm$
8:   **return** P_k

C TOPOLOGYFINDER Details

We first provide the mathematical foundation of the ring permutation rule.

Theorem 1 (Ring Generation). *For a cluster of N nodes $V = \{S_0, S_1, \cdots, S_{N-1}\}$, all integer numbers $p < N$, where p is co-prime with N (i.e. $gcd(p, N) = 1$) represent a unique ring-AllReduce permutation rule.*

Proof. Consider the integer modulo N group with addition $\mathbb{Z}_N^+ = \{0, 1, \cdots, (N-1)\}$. $\mathbb{Z}_N^+$ is a cyclic group. By fundamental theorem of cyclic groups, p is a generator of $\mathbb{Z}_N^+$ if and only if $gcd(p, N) = 1$. Hence we can cover the entire $\mathbb{Z}_N^+$ by repeatedly adding p to itself.

Now consider the graph $G_{\mathbb{Z}_N^+, p} = (V_{\mathbb{Z}_N^+}, E_p)$ where the set of vertices $V_{\mathbb{Z}_N^+} = \mathbb{Z}_N^+$ and $E_p = \{(a \times p, (a+1) \times p) \in V_{\mathbb{Z}_N^+}^2, a \in \mathbb{Z}_N^+\}$. The set E_p forms a cycle on $G_{\mathbb{Z}_N^+, p}$. Now denote our cluster as $G = (V, E)$ where V is defined as above and E represents a set of directed links. Then $G_{\mathbb{Z}_N^+, p}$ is isomorphic to G, hence following the rule in E_p we can define a valid ring in G. Furthermore, since $\forall p_i \neq p_j$ we can guarantee that $(0, p_i) \in E_{p_i}$ and $(0, p_j) \notin E_{p_i}$, each p_i is guaranteed to describe a unique ring. □

Algorithms 2, 3 and 4 list the detailed pseudocodes of sub-modules in Algorithm 1, namely `TotientPerms`, `CoinChangeMod` and `TopPermutations`.

To extend our approach to other AllReduce algorithms, one way is to generalize TotientPerms (Algorithm 2) so that the E_p described in theorem 1 simply represents a *permutation* which we apply to the original node labeling, while keeping the edge relation, to create an isomorphic graph that describes the new AllReduce topology.

Algorithm 5 TOPOOPT-reconfig pseudocode

```
 1: procedure TOPOOPT-RECONFIG(V, T, d, L)
       ▷ Input V: Nodes in the network
       ▷ Input T: Unsatisfied traffic demand matrix
       ▷ Input d: Node degree limit
       ▷ Input L: Number of links between ordered node-pair, initially zero
       ▷ Output E: Allocated links, initially empty
          ▷ Initially, E is empty
 2:       E = {}
          ▷ Initially, each node has d available tx and rx interfaces
 3:       for v ∈ V do
 4:           available_tx[v] = d
 5:           available_rx[v] = d
       ▷ Create new links according to the demand list
 6:       while ∃i, j < |V| : i ≠ j, available_tx[v_i] > 0, available_rx[v_j] > 0 do
             ▷ allocate a direct connection for the highest demand pair
 7:           (v_1, v_2) = node-pair with highest demand in T
 8:           e = NewLink(v_1, v_2)
 9:           E = E ∪ {e}
             ▷ Increment the number of parallel links from v_1 to v_2
10:           L(v_1, v_2) += 1
             ▷ Scale the demand down by the number of links
11:           T(v_1, v_2) ×= 1/2
             ▷ Update available interfaces
12:           for v ∈ (v_1, v_2) do
13:               available_tx[v_1] −= 1
14:               available_rx[v_2] −= 1
                 ▷ Stop considering nodes with zero available interfaces
15:           if available_tx[v_1] == 0 then
16:               for u ∈ V do
17:                   Remove (v_1, u)'s entry from T
18:           if available_rx[v_2] == 0 then
19:               for u ∈ V do
20:                   Remove (u, v_2)'s entry from T
21:       return E
```

D TOPOOPT-reconfig Heuristic

Algorithm 5 describes the heuristic we use for TOPOOPT-reconfig. As mentioned in Section 3.3, our goals are: (*i*) have enough bandwidth for large transfer demands; (*ii*) while also minimize the latency of indirect routing for nodes that do not have a direct link between them.

To achieve this goal in a reconfigurable interconnect, we propose a utility function that finds a balance between the two goals by maximizing the number of parallel links between high demand nodes but with a *diminishing return*. More formally, assume a network topology is represented by graph $G = (V, E)$ and each node has degree d. We define $L(i, j)$ to

be the number of parallel links between node-pair (i, j). Let $T(i, j)$ be the amount of unsatisfied traffic demand, we define a topology G's utility function as follows:

$$Utility(G) = \sum_{\{i,j\} \in E} T(i, j) \times Discount(L(i, j)) \tag{1}$$

The *Discount* function can be defined in different ways; in Algorithm 5 as well as Algorithm 1's MP construction, we use

$$Discount(l) = \sum_{x=1}^{l} 2^{-x} \tag{2}$$

to reduce the utility of additional links exponentially. One can also explore other discount scaling, such as linear or factorial functions.

When the fabric is reconfigurable (as in TOPOOPT-reconfig), we collect the unsatisfied traffic demand every 50 ms and run Algorithm 5 to decide the new network topology. After the new topology is computed, we pause all the flows for 10 ms representing the reconfiguration delay of the OCS, apply the new topology, and then resume the flows that has one or more corresponding physical links across the flow source and destination.

E Modifications to SiP-ML

Since SiP-ML's SiP-Ring proposal is based on a physical ring topology, its reconfiguration algorithm has several constraints about wavelength allocation for adjacent nodes. Given that TOPOOPT's physical topology is not a ring, directly applying SiP-Ring's optimization using their original C++ code have resulted SiP-ML to perform extremely poorly in our setup. To give SiP-ML a leg up, we observe that its formulation tries to optimize a utility function very similar to Equation 1 without the *Discount* part (i.e. *Discount* = 1), but with an ILP. While an ILP gives the optimal solution, its runtime makes it prohibitive for the amount of simulation parameters we explore. Therefore, we substitute the ILP with Algorithm 5 with *Discount* = 1 which is a heuristic that tries to achieve a similar goal.

Note that SiP-ML paper has another design called SiP-OCS, which is more similar architecturally to TOPOOPT. In the SiP-ML paper, SiP-OCS is proposed as a one-shot reconfiguration approach due to the long reconfiguration latency of 3D-MEMS based OCSs.